A MATHEMATICAL FRAMEWORK FOR DATA FABRICS

T. SHASKA

Abstract. We propose a mathematical framework for data fabrics, unifying heterogeneous data management in distributed systems through a hypergraph-based structure $\mathcal{F} = (D, M, G, T, P, A)$. Datasets, metadata, transformations, policies, and analytics are modeled over a distributed system $\Sigma = (N, C)$, with multi-way relationships encoded in a hypergraph $G = (V, E)$. A categorical approach, with datasets as objects and transformations as morphisms, supports operations like data integration and federated learning. The hypergraph is embedded into a modular tensor category, capturing relational symmetries via braided monoidal structures. We address NP-hard challenges, such as schema matching and partitioning, using spectral methods and symmetry-based alignments, ensuring consistency and scalability. Applied to a multi-component architecture, the framework supports real-time analytics with vector representations in $\mathbb{R}^{11}$. Future work explores dynamic categories and topological invariants, establishing data fabrics as a cornerstone for large-scale data ecosystems.

Contents

1. Introduction

The rapid proliferation of data from cloud computing, the Internet of Things (IoT), artificial intelligence (AI), and distributed systems has overwhelmed traditional data management frameworks. Centralized architectures, reliant on rigid schemas, struggle to integrate heterogeneous datasets, scale across distributed nodes, enforce governance, or support real-time analytics. For instance, IoT systems generating terabytes of sensor data daily require dynamic orchestration to unify diverse sources, ensure security, and deliver timely insights, a challenge unmet by conventional databases. Data fabrics address these issues by providing a unified, metadata-driven architecture that intelligently manages complex data ecosystems, enabling seamless integration, navigation, and analytics. This paper formalizes the data fabric as a mathematical structure, offering a rigorous, scalable framework to design adaptive, secure systems for modern data-driven applications.

We define the data fabric as a tuple $\mathcal{F} = (D, M, G, T, P, A)$, operating over a distributed system $\Sigma = (N, C)$, with components:

- D: Time-indexed datasets, capturing sources like IoT sensor readings or financial transactions.
- M: Metadata, providing context and transformation histories for discovery and provenance.
- G: A hypergraph, encoding multi-way relationships among datasets and metadata.

Date: June 29, 2025.

- T: Transformations, mapping data across domains for integration and processing.
- P: Governance policies, ensuring security and compliance via access control.
- A: Analytical functions, generating insights through statistical or machine learning models.
- Σ: A distributed system of nodes N and communication links C, hosting and processing data.

This framework, illustrated in **??**, leverages a hypergraph $G = (V, E)$ to model complex dependencies, a categorical structure $\mathcal{DF}$ to unify operations, and a modular tensor category (MTC) to capture relational symmetries via braided monoidal structures.

Our contributions span theoretical and practical advancements in data fabric design. We formalize the data fabric as a mathematical tuple $\mathcal{F}$, integrating datasets, metadata, and analytics within a hypergraph G. This hypergraph is embedded into a modular tensor category (MTC), capturing complex relational symmetries through braided monoidal structures, with novel geometric analogies to Hurwitz spaces that enrich its algebraic modeling, as detailed in Section 5.

To unify data fabric operations, we introduce a categorical structure $\mathcal{DF}$, modeling datasets as objects and transformations as morphisms. This approach provides a rigorous framework for operations such as data integration and federated learning, ensuring operational coherence across distributed systems, as explored in Section 4.

We also address computational challenges by proving the NP-hardness of critical tasks, including schema matching (theorem 3) and dynamic partitioning (theorem 29). To mitigate these bottlenecks, we propose spectral methods and symmetry-based alignments, offering scalable solutions for large-scale data management, as analyzed in Section 8.

For distributed system robustness, we ensure consistency, completeness, and causality under the CAP and CAL theorems. By leveraging hypergraph redundancy and MTC braiding, we design fault-tolerant operations that maintain coherence in dynamic, partitioned environments, as demonstrated in Section 9.

Practically, we apply the framework to a multi-component architecture, integrating databases, real-time analytics, and transformation pipelines. This system supports scalable operations with vector representations in $\mathbb{R}^{11}$, demonstrated through a real-world Amazon seller scenario, as presented in Section 10.

The paper is organized as follows. In Section 2, we define the data fabric tuple $\mathcal{F}$ and the distributed system Σ, formalizing components such as time-indexed datasets D, metadata M, and the hypergraph G with mathematical precision. Section 3 details core operations, including data integration, metadata-driven navigation, and federated learning, and establishes their computational complexities, proving challenges like the NP-hardness of schema matching. Section 4 introduces the categorical structure $\mathcal{DF}$, modeling datasets as objects and transformations as morphisms to provide a unified framework for these operations. Section 5 describes the hypergraph G, its vector representations in $\mathbb{R}^{11}$, and its embedding into a modular tensor category, drawing novel geometric analogies to Hurwitz spaces. In Section 8, we analyze computational bottlenecks, such as NP-hard partitioning, and propose mitigation strategies like spectral clustering and symmetry-based alignments. Section 9 examines consistency, completeness, and causality in distributed environments, leveraging the CAP and CAL theorems to ensure robust operations. Section 10 applies the framework to a multi-component architecture, integrating databases, real-time analytics, and transformation pipelines, with a practical demonstration through an Amazon seller scenario. Finally, Section 12 summarizes the paper's contributions and outlines future directions, exploring extensions like dynamic monoidal categories and topological invariants.

Symbol	**Description**
$\mathcal{F} = (D, M, G, T, P, A)$	Data fabric tuple
$G = (V, E)$	Hypergraph with vertices $V = D \cup M$, hyperedges E
$\mathcal{DF}$	Data fabric category, with datasets as objects, transformations as morphisms
$\Sigma = (N, C)$	Distributed system with nodes N, links C
Ω_i	Domain of dataset $d_i(t)$

TABLE 1. Key notation for the data fabric framework.

This work empowers researchers and practitioners to build adaptive, secure, and scalable data fabrics, addressing the complexities of modern data ecosystems while advancing theoretical foundations through rigorous mathematics.

2. An Introduction to Data Fabrics

The rapid expansion of data from cloud computing, the Internet of Things (IoT), artificial intelligence (AI), and distributed systems has outpaced traditional data management frameworks. Centralized or schema-rigid systems struggle to integrate heterogeneous datasets, scale across distributed nodes, enforce governance, or support real-time analytics. A data fabric offers a unified, metadata-driven architecture to manage diverse data assets intelligently, enabling seamless integration, navigation, and analytics. This section formalizes the data fabric as a mathematical structure, detailing its components and laying the foundation for operations (Section 3), categorical formalization (Section 4), and computational challenges (Section 8).

We define the data fabric as a tuple $\mathcal{F} = (D, M, G, T, P, A)$, operating over a distributed system $\Sigma = (N, C)$. The tuple $\mathcal{F}$ encapsulates data assets, metadata, relationships, transformations, policies, and analytics, while Σ models the distributed infrastructure. Below, we explore each component through mathematical formulations, practical examples (e.g., Amazon seller, healthcare), and visualizations, concluding with a formal definition and summary table.

2.1. Data Assets.

Data assets, denoted $D = \{d_i(t)\}_{i,t}$, form the core of the data fabric, representing time-indexed datasets critical for applications like IoT monitoring or e-commerce analytics. Each dataset $d_i(t)$ at time t is characterized by a schema S_i, defining its structure (e.g., attributes like price, timestamp), and a domain Ω_i, which is numerical ($\Omega_i \subseteq \mathbb{R}^k$) or categorical (e.g., {electronics, clothing}). Formally, $d_i(t) : T \to \Omega_i$, where $T \subseteq \mathbb{R}_{\geq 0}$ is the time domain, maps timestamps to data points.

For example, in an Amazon seller fabric, a sales dataset $d_1(t)$ might have schema $S_1 = \{\text{product-id} : \text{string}, \text{price} : \text{float}, \text{quantity} : \text{int}\}$, with domain $\Omega_1 = \mathbb{R} \times \mathbb{N}$. In a healthcare fabric, a patient record dataset $d_2(t)$ could have $S_2 = \{\text{patient-id} : \text{string}, \text{temperature} : \text{float}, \text{timestamp} : \text{datetime}\}$, with $\Omega_2 = \mathbb{R}$. The time-indexed nature of D supports streaming data, enabling real-time analytics (Section 8.4).

Heterogeneity across schemas S_i and domains Ω_i complicates integration. To quantify this, we define a schema distance metric:

$$\text{dist}(S_i, S_j) = \sum_{a \in S_i, b \in S_j} w(a, b) \cdot (1 - \text{sim}(a, b)),$$

where $\text{sim}(a, b) \in [0, 1]$ measures attribute similarity (e.g., via ontology alignment), and $w(a, b)$ weights importance. For instance, consider schemas $S_1 = \{\text{price}, \text{quantity}\}$ (sales) and $S_2 = \{\text{cost}, \text{stock}\}$ (inventory). Suppose $\text{sim}(\text{price}, \text{cost}) = 0.9$, $\text{sim}(\text{quantity}, \text{stock}) = 0.8$, $\text{sim}(\text{price}, \text{stock}) = 0.1$, $\text{sim}(\text{quantity}, \text{cost}) = 0.2$, and weights $w = 1$. The distance is:

$$\text{dist}(S_1, S_2) = (1 - 0.9) + (1 - 0.1) + (1 - 0.2) + (1 - 0.8) = 0.1 + 0.9 + 0.8 + 0.2 = 2.0.$$

This metric guides integration strategies (Section 3) but highlights NP-hard matching challenges (Section 8.1).

2.2. Metadata.

Metadata, $M = \{m_1, \ldots, m_k\}$, provides context for data assets, enabling discovery, navigation, and provenance tracking. Each $m_j = (d_i, \alpha_j, \tau_j)$ associates a dataset $d_i \in D$ with attributes $\alpha_j \subseteq \mathcal{A}$ (e.g., {source, format}) and a transformation history $\tau_j : D \to \mathcal{H}$, where $\mathcal{H}$ is a set of tuples (t_k, t_{apply}), with $t_k \in T$ a transformation (Section 2.4) and t_{apply} its timestamp.

For example, in a healthcare fabric, metadata m_1 for patient records $d_2(t)$ might include $\alpha_1 = \{\text{hospital} : \text{Mercy}, \text{date} : 2025-04-01\}$ and $\tau_1(d_2) = \{(t_1, 2025-04-01), (t_2, 2025-04-02)\}$, where t_1 cleans data and t_2 aggregates vitals. fig. 1 illustrates this transformation sequence.

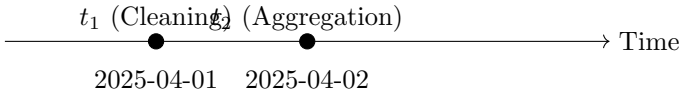

FIGURE 1. Timeline of transformations in $\tau_1(d_2)$, showing cleaning and aggregation applied to patient records.

Metadata links datasets via the hypergraph G (**??**) and tracks provenance (Section 3.5). Dynamic updates to M, especially for streaming $d_i(t)$, have complexity proportional to $|M| \cdot |T|$, impacting real-time processing (Section 8.4).

2.3. **Hypergraph.** The hypergraph $G = (V, E)$ models relationships among data and metadata, with vertices $V = D \cup M$ and hyperedges $E \subseteq \mathcal{P}(V)$. Unlike simple graphs, hyperedges connect multiple vertices, capturing complex dependencies. Formally, G is a directed hypergraph, where each hyperedge $e = (T_e, H_e)$ has a tail $T_e \subseteq V$ (inputs) and head $H_e \subseteq V$ (outputs). The adjacency set is:

$$\mathrm{Adj}(v) = \{e \in E \mid v \in T_e \cup H_e\}.$$

For example, in an Amazon seller fabric, a hyperedge $e = (\{d_1, m_1\}, \{d_3\})$ links a sales dataset d_1, metadata m_1 (e.g., category: electronics), and a derived dataset d_3 (e.g., aggregated sales), indicating a transformation. fig. 2 illustrates this.

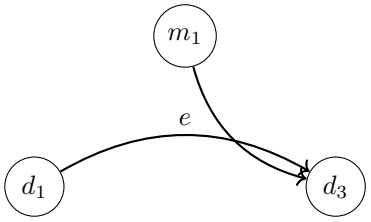

FIGURE 2. Example hyperedge in G, linking sales dataset d_1, metadata m_1, and derived dataset d_3.

The hypergraph enables metadata-driven navigation and provenance tracking (Section 3), but its size ($|V|$, $|E|$) and dynamic updates pose scalability challenges (Section 8.2).

2.4. **Transformations.** Transformations $T = \{t_1, \ldots, t_m\}$ are functions $t_i : \Omega_i \to \Omega_j$, mapping data across domains for integration, normalization, or aggregation. For example, in an IoT fabric, $t_1 : \mathbb{R} \to \{\text{low}, \text{high}\}$ converts temperature readings (e.g., $\geq 30°\text{C} \to$ high).

Each transformation satisfies:

$$t_i(d_i(t)) \in \Omega_j, \quad \text{loss}(t_i, d_i) = I(d_i; d_i) - I(t_i(d_i); d_i) \leq \epsilon,$$

where I is mutual information and $\epsilon > 0$ bounds loss. The cost $\text{cost}(t_i)$ varies (e.g., $O(n)$ for linear, $O(n^2)$ for complex mappings). Optimization balances efficiency and fidelity:

$$\min_{t_i \in T} \text{cost}(t_i) + \lambda \text{loss}(t_i, d_i),$$

with $\lambda > 0$. For instance, transforming sales quantities to stock levels minimizes loss by aligning units. Transformations are pivotal for integration and federated learning (Section 3), but their NP-hard selection complicates implementation (Section 8.1).

2.5. **Governance Policies.** Governance policies $P = \{p_1, \ldots, p_l\}$ enforce security and compliance, where each $p_i = (c_i, a_i)$ includes a predicate $c_i : D \times \mathcal{U} \to \{0, 1\}$ (e.g., user clearance) and action a_i (e.g., grant access). The user context space $\mathcal{U}$ includes roles or timestamps.

A request $r(d_i, u)$ is granted if:

$$r(d_i, u) = 1 \iff \bigwedge_{p_j = (c_j, a_j) \in P} c_j(d_i, u).$$

For example, in a financial fabric, $c_1(d_1, u) = 1$ if u is a trader accessing sales data d_1. Policies may enforce differential privacy for analytics (Section 3). Evaluation scales as $O(|P| \cdot |N|)$, posing challenges in large Σ (Section 8.3).

2.6. **Analytical Functions.** Analytical functions $A = \{a_1, \ldots, a_p\}$ generate insights, where $a_i : D \to \mathbb{R}^k$ (e.g., regression) or $\mathcal{C}$ (e.g., classification). For instance, in an Amazon seller fabric, $a_1(d_1)$ predicts sales trends from $d_1(t)$.

Each a_i is parameterized by θ_i, optimized via:

$$\theta_i = \arg\min_{\theta} \mathcal{L}(a_i(D, \theta), y),$$

where $\mathcal{L}$ is a loss function (e.g., mean squared error). For federated learning (Section 3), a_i operates locally, aggregating results. Complexity, often $O(|\theta_i| \cdot |D|)$, and concept drift in streaming data challenge real-time analytics (Section 8.4).

2.7. **Distributed System.** The distributed system $\Sigma = (N, C)$ hosts the fabric, with nodes N storing $D_n \subseteq D$ and links $C \subseteq N \times N$. The adjacency matrix is:

$$A_\Sigma(n_i, n_j) = \begin{cases} w(n_i, n_j) & \text{if } (n_i, n_j) \in C, \\ \infty & \text{otherwise,} \end{cases}$$

where $w(n_i, n_j)$ is latency or bandwidth. For example, in a cloud fabric, N includes data centers, and C models network links. Load balancing:

$$\text{load}(n) = |D_n| + \sum_{a_i \in A_n} \text{cost}(a_i),$$

is critical for scalability (Section 8.2).

2.8. **Formal Definition of a Data Fabric.** We define a data fabric as follows:

Definition. 1 (Data Fabric)**.** *A* data fabric *is a tuple* $\mathcal{F} = (D, M, G, T, P, A)$ *over* $\Sigma = (N, C)$*, where:*

(1) $D = \{d_i(t)\}_{i,t}$*: Time-indexed datasets with schemas* S_i *and domains* Ω_i *(Section 2.1).*
(2) $M = \{m_1, \ldots, m_k\}$*: Metadata* $m_j = (d_i, \alpha_j, \tau_j)$ *for context and history (Section 2.2).*
(3) $G = (V, E)$*: Directed hypergraph with* $V = D \cup M$*,* $E \subseteq \mathcal{P}(V)$ *(??).*
(4) $T = \{t_1, \ldots, t_m\}$*: Transformations* $t_i : \Omega_i \to \Omega_j$ *with loss constraints (Section 2.4).*
(5) $P = \{p_1, \ldots, p_l\}$*: Policies* $p_i = (c_i, a_i)$ *for compliance (Section 2.5).*
(6) $A = \{a_1, \ldots, a_p\}$*: Analytical functions parameterized by* θ_i *(Section 2.6).*
(7) $\Sigma = (N, C)$*: Distributed system hosting* $D_n \subseteq D$ *(Section 2.7).*

Conditions:

i) ***Consistency****:* $\tau_j(d_i) \subseteq \{(t_k, t_{apply}) \mid t_k \in T\}$.
ii) ***Connectivity****:* G *ensures paths from* $d_i \in D$ *to* $m_j \in M$.
iii) ***Compliance****:* $r(d_i, u) = 1 \iff \bigwedge_{p_j \in P} c_j(d_i, u)$.
iv) ***Distributivity****:* $D = \bigcup_{n \in N} D_n$*, with local processing and aggregation.*

table 2 summarizes the components.

Component	Description	Example
D	Time-indexed datasets	Sales records (S_1)
M	Metadata with history	Hospital, date for records
G	Hypergraph of relationships	$e = (\{d_1, m_1\}, \{d_3\})$
T	Transformations across domains	Convert temperature to alerts
P	Governance policies	Access control for traders
A	Analytical functions	Sales trend prediction
Σ	Distributed nodes and links	Cloud data centers

TABLE 2. Summary of Data Fabric Components

3. Operations of Data Fabrics

up to the relevant subsections The functionality of a data fabric, defined by the tuple $\mathcal{F} = (D, M, G, T, P, A)$ over the distributed system $\Sigma = (N, C)$ (Section 2), is realized through operations that leverage its components to manage and analyze distributed data. These operations—data integration, metadata-driven navigation, scalability and distribution, governance and security, provenance tracking, and federated learning—enable the fabric to address complex demands, such as merging heterogeneous datasets in e-commerce or ensuring privacy in healthcare. Each operation is rigorously formulated, grounded in the hypergraph G, transformations T, and analytical functions A, but their computational complexity poses challenges like NP-hard optimizations and latency constraints (Section 8). This section provides formal definitions, detailed proofs, complexity analyses, and illustrative examples from an Amazon seller fabric, with fig. 3 showing operation interactions and table 3 summarizing key properties.

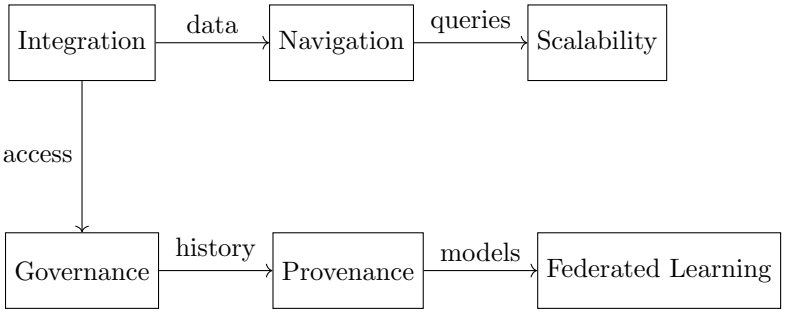

Figure 3. Interactions between data fabric operations, illustrating data flow from integration to federated learning.

3.1. Data Integration.

Definition. 2 (Data Integration)**.** Data integration *is a mapping* $\phi : D \to D' \subseteq D$*, where* D' *is a unified dataset, constructed by selecting transformations* $t \in T$ *such that for each* $d_i, d_j \in D$*,* $t(d_i) \in \Omega_j$*, satisfying schema compatibility and minimizing integration cost.*

Formally, for datasets $d_i, d_j \in D$, we seek a transformation $t \in T$ minimizing:

$$\min_{t \in T} \left(\sum_{d_i, d_j \in D} \text{dist}(S_i, t(S_j)) + \lambda \text{cost}(t) \right),$$

subject to:

$$t(d_i) \in \Omega_j, \quad \text{compat}(S_i, t(S_j)) \geq \theta,$$

where:

(1) $\text{dist}(S_i, S_j) = \sum_{a \in S_i, b \in S_j} w(a, b) \cdot (1 - \text{sim}(a, b))$ is the schema distance (Section 2.1),
(2) $\text{cost}(t)$ is the computational complexity of applying t (e.g., $O(n)$ for linear mappings, $O(n^2)$ for complex joins),
(3) $\lambda > 0$ balances schema alignment and computational efficiency,
(4) $\text{compat}(S_i, S_j) \in [0, 1]$ measures semantic compatibility via ontology mappings,
(5) $\theta \in (0, 1]$ is a compatibility threshold ensuring meaningful alignment.

The term *schema matching* refers to finding a mapping $\pi : S_i \to S_j$ that maximizes attribute similarity:

$$\max_{\pi : S_i \to S_j} \sum_{a \in S_i} \text{sim}(a, \pi(a)),$$

where $\text{sim}(a, b) \in [0, 1]$ is the similarity score. This process is central to integration but computationally challenging due to its NP-hard nature.

Theorem 3. *Schema matching, maximizing* $\sum_{a \in S_i} sim(a, \pi(a))$*, is NP-hard.*

Proof. We prove NP-hardness by reducing the subgraph isomorphism problem, known to be NP-hard, to schema matching. Let $G_1 = (V_1, E_1)$ and $G_2 = (V_2, E_2)$ be graphs with $|V_1| \leq |V_2|$, where we seek a subgraph of G_2 isomorphic to G_1. Construct schemas S_i and S_j as follows:

- For each vertex $v \in V_1$, create an attribute $a \in S_i$; for each vertex $v' \in V_2$, create an attribute $b \in S_j$.
- Define similarity: $\text{sim}(a, b) = 1$ if there exists a bijective mapping $\pi : S_i \to S'_j \subseteq S_j$ such that for all $(v, w) \in E_1$, there is a corresponding edge $(\pi(v), \pi(w)) \in E_2$, and $\pi(a) = b$; otherwise, $\text{sim}(a, b) = 0$.

Maximizing

$$\sum_{a \in S_i} \text{sim}(a, \pi(a))$$

requires finding a mapping π that aligns S_i with a subset of S_j, equivalent to finding a subgraph in G_2 isomorphic to G_1. The reduction is polynomial, as constructing S_i, S_j, and the similarity function takes

$$O(|V_1| + |V_2| + |E_1|).$$

Since subgraph isomorphism is NP-hard, schema matching is NP-hard. The decision version (does a mapping exist with similarity $\geq k$?) is in NP, as verifying a mapping takes polynomial time. □

Example 1. *To clarify the reduction, consider a subgraph isomorphism problem with* G_1 *as a triangle with*

$$V_1 = \{v_1, v_2, v_3\}, \quad E_1 = \{(v_1, v_2), (v_2, v_3), (v_3, v_1)\}$$

and G_2 *with*

$$V_2 = \{u_1, u_2, u_3, u_4\}, \quad E_2 = \{(u_1, u_2), (u_2, u_3), (u_3, u_1), (u_3, u_4)\}.$$

Construct schemas $S_i = \{a_1, a_2, a_3\}$ *corresponding to* v_1, v_2, v_3*, and* $S_j = \{b_1, b_2, b_3, b_4\}$ *for* u_1, u_2, u_3, u_4*. The similarity* $sim(a_i, b_j) = 1$ *if mapping* $a_i \to b_j$ *preserves* G_1*'s edge structure in* G_2*, else 0. Maximizing*

$$\sum_{a \in S_i} sim(a, \pi(a))$$

finds a mapping $\pi : \{a_1, a_2, a_3\} \to \{b_1, b_2, b_3\}$ *if* u_1, u_2, u_3 *form a triangle in* G_2*, mirroring the subgraph isomorphism task.*

Lemma 1. *Approximating schema matching within a constant factor is NP-hard.*

Proof. The subgraph isomorphism problem lacks a constant-factor approximation unless P = NP, as small changes in edge mappings drastically reduce isomorphism. Since the reduction preserves this property with binary similarity ($\text{sim}(a, b) \in \{0, 1\}$), approximating $\sum_{a \in S_i} \text{sim}(a, \pi(a))$ within a constant factor remains NP-hard. □

Example 2. *For practical integration in an Amazon seller fabric, consider integrating a sales dataset* $d_1(t)$ *with schema* $S_1 = \{product\text{-}id, price, quantity\}$*, domain* $\Omega_1 = \mathbb{R} \times \mathbb{N}$*, and an inventory dataset* $d_2(t)$ *with* $S_2 = \{product\text{-}id, cost, stock\}$*,* $\Omega_2 = \mathbb{R} \times \mathbb{N}$*. A transformation* $t_1 \in T$ *aligns attributes (e.g.,* $t_1 : price \to cost$ *via scaling), producing a unified dataset* $d_3(t)$ *with schema* $S_3 = \{product\text{-}id, price, quantity, stock\}$*. The schema distance* $dist(S_1, S_2)$*, as defined in Section 2.1, guides the choice of* t_1*, but the NP-hardness of schema matching necessitates heuristic algorithms for large datasets (Section 8.1).*

The non-commutative nature of transformation compositions, where $t_1 \circ t_2 \neq t_2 \circ t_1$, mirrors the algebraic structure of quantum groups, such as $U_q(\mathfrak{sl}_2)$, whose coproduct defines non-commutative tensor products. This analogy suggests that quantum group actions could model order-sensitive dependencies in integration, potentially informing optimization strategies for selecting $t_i \in T$, as explored in Section 8.1.

3.2. **Metadata-Driven Navigation.**

Definition. 4 (Metadata-Driven Navigation)**.** Metadata-driven navigation *resolves a query* $q : D \to \{0, 1\}$ *by traversing* G*, finding the shortest path* $p \in Paths(v_s, v_t)$ *from a source vertex* $v_s \in V$ *(e.g., metadata) to a target vertex* $v_t \in V$ *(e.g., dataset), minimizing the path cost:*

$$argmin_{p \in Paths(v_s, v_t)} \sum_{(u,v) \in p} w(u, v),$$

where $w(u, v) \geq 0$ *reflects latency or semantic distance.*

Paths in G are sequences of hyperedges $e_1, e_2, \ldots$, where $H_{e_i} \cap T_{e_{i+1}} \neq \emptyset$. Navigation employs a modified Dijkstra's algorithm, adapted for hypergraphs as follows:

(1) Initialize a priority queue with $(v_s, 0)$, setting distances $\text{dist}[v] = \infty$ except $\text{dist}[v_s] = 0$.
(2) For each vertex u, explore hyperedges $e = (T_e, H_e) \in \text{Out}(u)$, updating $\text{dist}[v]$ for $v \in H_e$ if $\text{dist}[u] + w(u, v) < \text{dist}[v]$.
(3) Use a sparse representation of G, with $|E| = O(|V| \log |V|)$, yielding complexity $O(|E| + |V| \log |V|)$, as edge traversals dominate and the priority queue uses logarithmic updates.

The complexity arises from processing each hyperedge ($O(|E|)$) and updating distances via a priority queue ($O(|V| \log |V|)$), assuming efficient access via compressed sparse row formats. Dynamic updates to G, such as adding new datasets or metadata, increase computational overhead, impacting scalability (Section 8.2).

For example, in an Amazon seller fabric, a query $q(d_i) = (\text{category} = \text{electronics} \wedge \text{quantity} > 100)$ starts at a metadata vertex $m_1 \in M$ with attributes $\alpha_1 = \{\text{category} : \text{electronics}\}$. The navigation traverses a hyperedge $e_1 = (\{m_1\}, \{d_1\})$ to a sales dataset $d_1(t)$, followed by $e_2 = (\{d_1, m_2\}, \{d_3\})$ to an aggregated dataset $d_3(t)$, where m_2 includes time constraints (e.g., $\alpha_2 = \{\text{date} : 2025 - 04 - 01\}$). Assigning weights $w(u, v) = 1$ for simplicity, the path cost is 2, representing the number of hyperedges traversed.

3.3. **Scalability and Distribution.**

Definition. 5 (Scalability and Distribution)**.** Scalability and distribution *partitions the data assets* $D = \bigcup_{n \in N} D_n$*, where* $D_n \subseteq D$ *resides on node* $n \in N$*, and computes analytics* $a \in A$ *as an aggregation:*

$$a(D) = \bigoplus_{n \in N} a(D_n),$$

while minimizing computational and communication costs.

Formally, the partitioning problem seeks to minimize:

$$\min_{\{D_n\}} \left(\sum_{n \in N} \text{cost}(a(D_n)) + \sum_{(n_i, n_j) \in C} \text{comm}(D_{n_i}, D_{n_j}) \right),$$

where:

(1) $\text{cost}(a(D_n)) = O(|D_n|)$ is the computational cost of analytics on D_n,
(2) $\text{comm}(D_{n_i}, D_{n_j})$ is the communication cost, proportional to the data transfer size across the link $(n_i, n_j) \in C$,
(3) $\bigoplus$ is an aggregation operator (e.g., sum for regression coefficients, union for classification labels).

For instance, in an Amazon seller fabric, a sales dataset $d_1(t)$ is partitioned across regional servers $\{D_{n_1}, D_{n_2}, \ldots\}$, where each node $n_i \in N$ computes a local sales total $a(D_{n_i}) = \sum_{x \in D_{n_i}} x.\text{quantity}$. These totals are aggregated globally via summation, yielding the total sales $a(D) = \sum_{n \in N} a(D_{n_i})$. The optimization balances local computation costs (linear in $|D_{n_i}|$) against communication costs, which depend on data dependencies across nodes.

The partitioning problem is NP-hard, as demonstrated by the following theorem.

Theorem 6. *The partitioning problem, minimizing* $\sum_{n \in N} \text{cost}(a(D_n)) + \sum_{(n_i, n_j) \in C} \text{comm}(D_{n_i}, D_{n_j})$*, is NP-hard.*

Proof. We reduce the graph partitioning problem, known to be NP-hard, to the data partitioning problem. Given a graph $G = (V, E)$ with edge weights $w(e)$, map vertices V to datasets D, edges E to data dependencies, and edge weights to communication costs comm. Assigning datasets D to nodes N to minimize inter-node communication corresponds to partitioning G to minimize the sum of edge weights crossing partitions, an NP-hard problem. The reduction is polynomial, as mapping vertices to datasets and edges to dependencies takes $O(|V| + |E|)$, confirming that the data partitioning problem is NP-hard. □

This computational complexity, further analyzed in Section 8.2, limits efficiency for dynamic datasets $d_i(t)$, necessitating adaptive partitioning strategies to balance load and minimize communication overhead.

3.4. **Governance and Security.**

Definition. 7 (Governance and Security)**.** Governance and security *enforces a set of policies* $P = \{p_1, \ldots, p_l\}$*, where each policy* $p_i = (c_i, a_i)$ *consists of a predicate* $c_i : D \times \mathcal{U} \to \{0, 1\}$ *and an action* a_i*, to grant access requests* $r(d_i, u)$ *and ensure privacy via mechanisms like differential privacy for analytics* $a \in A$*.*

A request $r(d_i, u)$ for dataset $d_i \in D$ by user context $u \in \mathcal{U}$ (e.g., role, credentials, timestamp) is granted if:

$$r(d_i, u) = 1 \iff \bigwedge_{p_j=(c_j,a_j)\in P} c_j(d_i, u).$$

The predicate $c_j(d_i, u)$ evaluates conditions such as user authorization or data sensitivity. For example, in an Amazon seller fabric, a manager u with role "admin" requests access to a sales dataset $d_1(t)$. The policy set P includes predicates like $c_1(d_1, u) = 1$ if u.role = admin, ensuring only authorized users access sensitive data.

Differential privacy protects individual data points in analytics, formalized as:

$$P(a(D) \mid D) \leq e^{\epsilon} P(a(D') \mid D') + \delta,$$

for neighboring datasets D, D' (differing by one record), with privacy parameters $\epsilon, \delta > 0$. For instance, computing the average sales across $d_1(t)$ in the Amazon seller fabric uses differential privacy to ensure individual transaction details are not revealed, maintaining customer privacy while providing aggregate insights.

Policy evaluation complexity is:

$$O(|P| \cdot |N|),$$

as each policy $p_j \in P$ is checked across all nodes N, assuming constant-time predicate evaluation (e.g., role or credential lookup). This scalability challenge is further explored in Section 8.3.

Theorem 8. *Policy evaluation for a request* $r(d_i, u)$ *has complexity* $O(|P| \cdot |N|)$*.*

Proof. To evaluate $r(d_i, u)$, compute the conjunction $\bigwedge_{p_j=(c_j,a_j)\in P} c_j(d_i, u)$ across nodes N. Each predicate c_j requires $O(1)$ operations, assuming constant-time context lookup (e.g., checking user roles or data attributes). With $|P|$ policies, evaluating all predicates on a single node takes $O(|P|)$. In a distributed system, verification may require checking d_i or policy conditions on each of the $|N|$ nodes, as data or policies may be distributed, yielding a worst-case complexity of $O(|P| \cdot |N|)$. □

3.5. **Provenance Tracking.**

Definition. 9 (Provenance Tracking)**.** Provenance tracking *constructs the trace of a dataset* $d_i \in D$*, defined as:*

$$\textit{trace}(d_i) = \{t_j \in T \mid t_j \textit{ was applied to produce or modify } d_i\},$$

using the transformation history $\tau_j : D \to \mathcal{H}$ *from metadata* $m_j \in M$ *and the hypergraph* G*.*

Formally, for a metadata descriptor $m_j = (d_i, \alpha_j, \tau_j) \in M$, the provenance is:

$$\text{trace}(d_i) = \{t_k \in T \mid (t_k, t_{\text{apply}}) \in \tau_j(d_i)\}.$$

The hypergraph G supports this by providing paths linking d_i, its metadata m_j, and source datasets through hyperedges. For example, in an Amazon seller fabric, tracing the provenance of a sales forecast dataset $d_6(t)$ involves identifying transformations $t_1 \in T$ (data cleaning) and $t_2 \in T$ (aggregation) applied to a raw sales dataset $d_1(t)$. The metadata $m_3 \in M$ contains $\tau_3(d_6) = \{(t_1, 2025-04-01), (t_2, 2025-04-02)\}$, and the hypergraph includes a hyperedge $e_1 = (\{d_1, m_2\}, \{d_6\})$, where m_2 records additional context (e.g., time range).

The complexity of provenance tracking is:

$$O(|T| \cdot |E|),$$

as reconstructing $\tau_j(d_i)$ requires traversing all hyperedges $e \in E$ for each transformation $t_k \in T$. Dynamic updates to T or G, such as new transformations or datasets in streaming scenarios, further impact real-time performance (Section 8.4).

Theorem 10. *Provenance tracking for a dataset* d_i *has complexity* $O(|T| \cdot |E|)$*.*

Proof. To compute trace(d_i), retrieve the transformation history $\tau_j(d_i)$ from the metadata $m_j \in M$, which lists up to $|T|$ transformations $t_k \in T$. Verifying each transformation t_k involves checking all hyperedges $e \in E$ where d_i appears in the tail T_e or head H_e, requiring $O(|E|)$ operations per transformation. With $|T|$ transformations, the total complexity is $O(|T| \cdot |E|)$. □

3.6. **Federated Learning.**

Definition. 11 (Federated Learning)**.** Federated learning *computes an analytical function $a \in A$ over distributed data $D = \bigcup_{n\in N} D_n$, where each node $n \in N$ trains a local model with parameters θ_n on local data D_n, and results are aggregated:*

$$a(D) = \bigoplus_{n\in N} a(D_n, \theta_n).$$

Local model parameters θ_n are updated via gradient descent:

$$\theta_n \leftarrow \theta_n - \eta \nabla \mathcal{L}(a(D_n, \theta_n)),$$

where $\eta > 0$ is the learning rate, and $\mathcal{L}$ is a loss function (e.g., cross-entropy for classification, mean squared error for regression). The global model aggregates local updates, typically through averaging:

$$\theta = \frac{1}{|N|} \sum_{n\in N} \theta_n.$$

For example, in an Amazon seller fabric, regional servers $n_i \in N$ train local models $a(D_{n_i}, \theta_{n_i})$ to predict sales trends based on local sales data $D_{n_i} \subset d_1(t)$. Each D_{n_i} contains sales records with attributes $\{\text{price}, \text{quantity}\}$, and the model outputs a predicted sales volume. The local parameters θ_{n_i} (e.g., neural network weights) are aggregated by averaging to form a global predictor θ, ensuring privacy as raw data remains local.

The computational complexity per iteration for local model training is:

$$O(|\theta_n| \cdot |D_n|),$$

reflecting the cost of gradient computation across $|D_n|$ data points, each requiring $O(|\theta_n|)$ operations for a model with $|\theta_n|$ parameters. Communication costs for aggregating θ_n across nodes are proportional to $|N| \cdot |\theta_n|$, as each node sends its parameter vector. Concept drift, where the data distribution $P(D_n)$ changes over time, is detected using statistical tests:

$$D = \sup_x |F_t(x) - F_{t'}(x)|,$$

where $F_t(x)$ and $F_{t'}(x)$ are cumulative distribution functions at times t and t'. Detection complexity is $O(|D_n| \log |D_n|)$, typically implemented via Kolmogorov-Smirnov tests. These challenges, including communication overhead and drift adaptation, are further analyzed in Section 8.4.

Theorem 12. *Local model training in federated learning has complexity $O(|\theta_n| \cdot |D_n|)$ per iteration.*

Proof. For each node $n \in N$, computing the gradient $\nabla \mathcal{L}(a(D_n, \theta_n))$ involves evaluating the analytical function $a(D_n, \theta_n)$ over $|D_n|$ data points. Each evaluation requires $O(|\theta_n|)$ operations for a model with $|\theta_n|$ parameters (e.g., computing forward and backward passes in a neural network). Updating θ_n via gradient descent is $O(|\theta_n|)$, as it involves vector operations on the parameters. Thus, the total complexity per iteration is $O(|\theta_n| \cdot |D_n|)$. □

3.7. **Summary of Operations.** table 3 summarizes the operations, their computational complexities, and illustrative examples from the Amazon seller fabric, providing a concise reference for their mathematical properties and practical applications.

Operation	**Complexity**	**Amazon Seller Example**
Data Integration	NP-hard	Unify sales and inventory schemas
Metadata-Driven Navigation	$O(\|E\| + \|V\| \log \|V\|)$	Query high-selling electronics
Scalability and Distribution	NP-hard	Partition sales across servers
Governance and Security	$O(\|P\| \cdot \|N\|)$	Authorize manager access to sales
Provenance Tracking	$O(\|T\| \cdot \|E\|)$	Trace sales forecast to raw data
Federated Learning	$O(\|\theta_n\| \cdot \|D_n\|)$	Predict sales trends regionally

TABLE 3. Summary of Data Fabric Operations, Complexities, and Examples

4. A Categorical Perspective

Category theory, a branch of mathematics that abstracts structures and their relationships into objects and morphisms, offers a powerful framework for unifying the operations of a data fabric. By modeling datasets as objects and transformations as morphisms, category theory provides a lens to analyze the interactions of data fabric components ($\mathcal{F} = (D, M, G, T, P, A)$, Section 2) and their operations (Section 3). This section introduces the fundamentals of category theory, formalizes the data fabric as a category $\mathcal{DF}$, and demonstrates how functorial mappings and natural transformations integrate operations and inform challenges like consistency and dynamic schema updates (Section 8). We provide rigorous definitions, theorems, and references to foundational works, culminating in a categorical unification of the data fabric framework.

4.1. Introduction to Category Theory.

Definition. 13 (Category). *A* category $\mathcal{C}$ *consists of:*

(1) A collection of objects $Ob(\mathcal{C})$.
(2) For each pair of objects $A, B \in Ob(\mathcal{C})$*, a set of* morphisms $Hom_{\mathcal{C}}(A, B)$.
(3) A composition *operation* $\circ : Hom_{\mathcal{C}}(B, C) \times Hom_{\mathcal{C}}(A, B) \to Hom_{\mathcal{C}}(A, C)$*, where for* $f : A \to B$, $g : B \to C$, *we have* $g \circ f : A \to C$.
(4) For each object A*, an* identity morphism $id_A : A \to A$.

These satisfy the following axioms:

(1) Associativity*: For* $f : A \to B$, $g : B \to C$, $h : C \to D$,

$$(h \circ g) \circ f = h \circ (g \circ f).$$

(2) Identity*: For* $f : A \to B$,

$$f \circ id_A = f, \quad id_B \circ f = f.$$

Theorem 14. *The composition operation in a category* $\mathcal{C}$ *is associative.*

Proof. By definition, for morphisms $f : A \to B$, $g : B \to C$, $h : C \to D$ in $\mathcal{C}$, the associativity axiom states $(h \circ g) \circ f = h \circ (g \circ f)$. This is a direct consequence of the category's structure, ensuring that the order of composition does not affect the result, as composition is defined to satisfy this property for all morphisms in $\mathrm{Hom}_{\mathcal{C}}$. □

Examples of categories include:

(1) **Set**: Objects are sets, morphisms are functions, composition is function composition, and identity morphisms are identity functions.
(2) **Graph**: Objects are graphs, morphisms are graph homomorphisms, composition is homomorphism composition, and identity morphisms preserve graph structure.
(3) **Top**: Objects are topological spaces, morphisms are continuous functions, with standard composition and identities.

Functors map between categories, preserving their structure, and are crucial for relating the data fabric to its hypergraph representation.

Definition. 15 (Functor). *A* functor $F : \mathcal{C} \to \mathcal{D}$ *between categories* $\mathcal{C}$ *and* $\mathcal{D}$ *assigns:*

(1) Each object $A \in Ob(\mathcal{C})$ *to an object* $F(A) \in Ob(\mathcal{D})$.
(2) Each morphism $f : A \to B$ *in* $\mathcal{C}$ *to a morphism* $F(f) : F(A) \to F(B)$ *in* $\mathcal{D}$,

such that:

(1) $F(g \circ f) = F(g) \circ F(f)$ *for* $f : A \to B$, $g : B \to C$,
(2) $F(id_A) = id_{F(A)}$ *for each* $A \in Ob(\mathcal{C})$.

Theorem 16. *A functor* $F : \mathcal{C} \to \mathcal{D}$ *preserves composition and identities.*

Proof. By definition, F satisfies $F(g \circ f) = F(g) \circ F(f)$ for morphisms $f : A \to B$, $g : B \to C$, ensuring composition is preserved. Similarly, $F(\mathrm{id}_A) = \mathrm{id}_{F(A)}$ preserves identity morphisms. These properties are axioms of the functor, directly guaranteed by its definition. □

Natural transformations provide a way to compare functors, modeling relationships between different representations of the data fabric.

Definition. 17 (Natural Transformation)**.** *A* natural transformation $\eta : F \to G$ *between functors* $F, G : \mathcal{C} \to \mathcal{D}$ *assigns to each object* $A \in Ob(\mathcal{C})$ *a morphism* $\eta_A : F(A) \to G(A)$ *in* $\mathcal{D}$*, such that for every morphism* $f : A \to B$ *in* $\mathcal{C}$*, the following diagram commutes:*

$$\begin{array}{ccc} F(A) & \xrightarrow{\eta_A} & G(A) \\ \Big\downarrow{\scriptstyle F(f)} & & \Big\downarrow{\scriptstyle G(f)} \\ F(B) & \xrightarrow{\eta_B} & G(B) \end{array}$$

i.e., $\eta_B \circ F(f) = G(f) \circ \eta_A$.

Category theory's abstraction is particularly suited to data fabrics, where datasets (D) can be objects, transformations (T) can be morphisms, and operations like integration and navigation can be modeled as compositions or functorial mappings. Foundational references include [?MacLane1971] for a comprehensive treatment, [?Awodey2010] for an accessible introduction, and [?Spivak2014] for applications to databases and data management.

4.2. Data Fabric as a Category.

Definition. 18 (Data Fabric Category)**.** *The* data fabric category $\mathcal{DF}$ *is defined as follows:*

(1) Objects*: $D = \{d_i(t)\}_{i,t}$, the time-indexed data assets (Section 2.1).*
(2) Morphisms*: $T = \{t_1, \ldots, t_m\}$, where $t_i : d_i \to d_j$ is a transformation $t_i : \Omega_i \to \Omega_j$ (Section 2.4).*
(3) Composition*: For $t_1 : d_i \to d_j$, $t_2 : d_j \to d_k$, the composite $t_2 \circ t_1 : d_i \to d_k$, defined by $(t_2 \circ t_1)(x) = t_2(t_1(x))$.*
(4) Identity*: For each $d_i \in D$, the identity morphism $id_{d_i} : d_i \to d_i$, where $id_{d_i}(x) = x$.*

Theorem 19. *$\mathcal{DF}$ is a category, with associative composition and identity morphisms.*

Proof. To verify $\mathcal{DF}$ is a category:

(1) *Associativity*: For morphisms $t_1 : d_i \to d_j$, $t_2 : d_j \to d_k$, $t_3 : d_k \to d_l$, composition is function composition: $(t_3 \circ t_2) \circ t_1(x) = t_3(t_2(t_1(x))) = t_3 \circ (t_2 \circ t_1)(x)$, which is associative by the associativity of function composition.
(2) *Identity*: For $t_i : d_i \to d_j$, the identity $\mathrm{id}_{d_i}(x) = x$ satisfies $t_i \circ \mathrm{id}_{d_i} = t_i$, as $t_i(\mathrm{id}_{d_i}(x)) = t_i(x)$, and similarly $\mathrm{id}_{d_j} \circ t_i = t_i$. For $\mathrm{id}_{d_j} : d_j \to d_j$, $\mathrm{id}_{d_j}(t_i(x)) = t_i(x)$.

Thus, $\mathcal{DF}$ satisfies the category axioms. □

For example, in a supply chain fabric, $d_i \in D$ is raw shipment data, d_j is normalized data, and d_k is an aggregated inventory summary. Transformations $t_1 : d_i \to d_j$ (normalization) and $t_2 : d_j \to d_k$ (aggregation) compose as $t_2 \circ t_1 : d_i \to d_k$, representing the full data processing pipeline.

The hypergraph G (Section 2.3) is modeled via a functor to the category of hypergraphs.

Definition. 20 (Hypergraph Category)**.** *The category $\mathcal{HG}$ has:*

(1) Objects*: Hypergraphs $G = (V, E)$, where V is a set of vertices, and $E \subseteq \mathcal{P}(V)$ is a set of hyperedges.*
(2) Morphisms*: Hypergraph homomorphisms $\phi : G_1 \to G_2$, where $\phi : V_1 \to V_2$ maps vertices such that for each $e \in E_1$, $\phi(e) = \{\phi(v) \mid v \in e\} \in E_2$.*
(3) Composition*: Standard function composition of homomorphisms.*
(4) Identity*: The identity morphism $id_G : G \to G$, where $id_G(v) = v$.*

A functor $F : \mathcal{DF} \to \mathcal{HG}$ maps the data fabric to its hypergraph representation:

(1) *Objects*: $d_i \in D \mapsto v_i \in V$, where v_i is a vertex in G.
(2) *Morphisms*: $t_i : d_i \to d_j \mapsto e \in E$, where $e = (T_e, H_e)$ with $T_e = \{v_i, m_k\}$, $H_e = \{v_j\}$, and $m_k \in M$ is metadata associated with t_i.

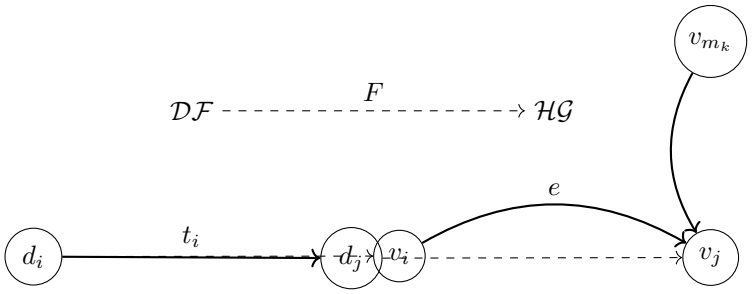

Functor $F : \mathcal{DF} \to \mathcal{HG}$, mapping datasets to vertices and transformations to hyperedges.

FIGURE 4. Categorical mapping of the data fabric to its hypergraph representation.

The functor preserves composition:

$$F(t_2 \circ t_1) = F(t_2) \circ F(t_1),$$

as a sequence $t_2 \circ t_1 : d_i \to d_k$ maps to a hyperedge path from v_i to v_k via v_j. For instance, $t_1 \circ t_2$ in a supply chain fabric corresponds to a path in G linking shipment data, inventory, and forecasts, enabling lineage tracking.

Theorem 21. *The functor $F : \mathcal{DF} \to \mathcal{HG}$ preserves composition and identities.*

Proof. For morphisms $t_1 : d_i \to d_j$, $t_2 : d_j \to d_k$, $F(t_1) = e_1 = (\{v_i, m_{k1}\}, \{v_j\})$, $F(t_2) = e_2 = (\{v_j, m_{k2}\}, \{v_k\})$. The composite $t_2 \circ t_1$ maps to a hyperedge path e_1, e_2, where $H_{e_1} \cap T_{e_2} = \{v_j\} \neq \emptyset$, represented as a composite morphism in $\mathcal{HG}$. Thus, $F(t_2 \circ t_1) = F(t_2) \circ F(t_1)$. For identity id_{d_i}, $F(\mathrm{id}_{d_i}) = \mathrm{id}_{v_i}$, the identity morphism in $\mathcal{HG}$, preserving identities. □

4.3. **Unifying Operations.** The categorical structure of $\mathcal{DF}$ and the functor F unify the operations of the data fabric (Section 3):

(1) *Data Integration*: Composes morphisms in $\mathcal{DF}$. For $t_1 : d_i \to d_j$, integration chains transformations to align schemas, minimizing schema distance (Section 3.1).
(2) *Metadata-Driven Navigation*: Traverses hyperedge paths in $\mathcal{HG}$ via F, finding shortest paths between datasets and metadata (Section 3.2).
(3) *Provenance Tracking*: Reconstructs morphism sequences in $\mathcal{DF}$, yielding $\mathrm{trace}(d_i)$ (Section 3.5).
(4) *Federated Learning*: Models local analytics as morphisms in $\mathcal{DF}$, with aggregation as a functorial operation across nodes (Section 3.6).

Consider a healthcare fabric: patient records d_i are transformed to normalized data d_j via t_1 (cleaning), then to predictions d_k via t_2 (model inference). The sequence $t_2 \circ t_1$ in $\mathcal{DF}$ maps to a hyperedge path in G, supporting integration (aligning records), navigation (locating related data), provenance (tracking transformations), and federated learning (distributed model training).

4.4. **Natural Transformations and Consistency.** Natural transformations model relationships between different functorial representations of the data fabric, addressing consistency constraints in distributed systems (Section 8).

Definition. 22 (Data Fabric Natural Transformation)**.** *A* natural transformation $\eta : F \to G$ *between functors $F, G : \mathcal{DF} \to \mathcal{HG}$ assigns to each dataset $d_i \in D$ a morphism $\eta_{d_i} : F(d_i) \to G(d_i)$ in $\mathcal{HG}$, such that for each transformation $t_i : d_i \to d_j$:*

$$\eta_{d_j} \circ F(t_i) = G(t_i) \circ \eta_{d_i}.$$

For example, F and G may map $\mathcal{DF}$ to different hypergraph representations of G (e.g., with different metadata granularity). The natural transformation η ensures that navigation paths (via F) align with transformation sequences (via G), maintaining consistency across distributed nodes $N \in \Sigma$. This is critical for operations like provenance tracking, where transformation histories must be consistent across representations.

Theorem 23. *Natural transformations $\eta : F \to G$ ensure commutative diagrams for data fabric operations.*

Proof. By definition, for $t_i : d_i \to d_j$, $\eta_{d_j} \circ F(t_i) = G(t_i) \circ \eta_{d_i}$. This ensures that the diagram in $\mathcal{HG}$ commutes, meaning that transformations in $\mathcal{DF}$ (mapped by F and G) preserve the relational structure of G. For operations like navigation, $F(t_i)$ and $G(t_i)$ represent hyperedge paths, and η ensures path equivalence, maintaining operational consistency. □

4.5. **Applications and Challenges.** The categorical perspective provides several benefits for data fabrics:

(1) *Unification*: Operations are abstracted as compositions or functorial mappings, simplifying their analysis and implementation.
(2) *Consistency*: Natural transformations model consistency constraints, ensuring alignment across distributed nodes (Section 8).
(3) *Scalability*: Functorial mappings to $\mathcal{HG}$ support efficient navigation and provenance tracking, though dynamic updates to $\mathcal{DF}$ (e.g., evolving schemas $S_i(t)$) pose challenges (Section 8.1).

For instance, in an IoT fabric, sensor data transformations are morphisms in $\mathcal{DF}$, mapped to hyperedges in G, enabling real-time analytics (Section 8.4). However, challenges like NP-hard schema matching (Section 8.1) and latency constraints (Section 8.4) require categorical extensions, such as dynamic categories or adjoint functors, as explored in [?Spivak2014].

The categorical approach also informs distributed system design by abstracting node interactions in Σ. Future work may leverage monoidal categories or topos theory to model governance policies P or analytical functions A, building on frameworks proposed in [?Schultz2016].

5. The Hypergraph: Vector Representations, Adjacency Structure, and Modular Tensor Categories

The hypergraph $G = (V, E)$, a fundamental component of the data fabric $\mathcal{F} = (D, M, G, T, P, A)$, encodes the relational and operational structure of data assets D and metadata M. Unlike the preliminary description in Section 2.3, this section provides a comprehensive mathematical treatment of three key aspects: the transformation of data assets into vector representations, the construction of the hypergraph's adjacency structure, and a precise embedding of the hypergraph into a modular tensor category (MTC). These developments build on the operations detailed in Section 3, such as data integration and navigation, and the categorical framework of Section 4, which models datasets as objects and transformations as morphisms. The MTC connection leverages a braided monoidal structure to capture the hypergraph's multi-way dependencies, drawing profound analogies with geometric structures like Hurwitz spaces and moduli spaces of covers, and suggesting links to topological data analysis and spectral graph theory for addressing computational challenges (Section 8). We preserve the full mathematical rigor of the framework, augment it with expanded proofs and a new lemma, and enhance presentation with visualizations in figs. 5 and 6, ensuring a robust foundation for scalable data fabric operations.

5.1. **Vector Representations of Data Assets.** To integrate data assets $D = \{d_i(t)\}_{i,t}$ into the hypergraph G and its categorical embedding, we represent each dataset $d_i(t)$, defined over a domain Ω_i with schema S_i, as a vector in a finite-dimensional space. This representation accommodates numerical, categorical, and mixed-type data, while accounting for temporal dynamics inherent in time-indexed datasets, supporting operations like integration (Section 3.1) and navigation (Section 3.2).

For numerical data, where $\Omega_i \subseteq \mathbb{R}^k$, a dataset $d_i(t)$ comprises a set of points $\{\mathbf{x}_1, \ldots, \mathbf{x}_n\}$, each $\mathbf{x}_j = (x_{j1}, \ldots, x_{jk}) \in \mathbb{R}^k$. Assuming Ω_i is convex, the representative vector is the centroid:

$$\mathbf{v}_i(t) = \frac{1}{n} \sum_{j=1}^{n} \mathbf{x}_j \in \mathbb{R}^k,$$

ensuring $\mathbf{v}_i(t) \in \Omega_i$. For non-convex Ω_i, alternatives such as the medoid:

$$\mathbf{v}_i(t) = \arg\min_{\mathbf{x}_j \in d_i(t)} \sum_{l=1}^{n} \|\mathbf{x}_j - \mathbf{x}_l\|_2,$$

or a convex hull approximation are employed, with medoid computation requiring $O(n^2 k)$. This vector preserves the dataset's central tendency, facilitating similarity computations in hypergraph operations.

For categorical data, where $\Omega_i = \{c_1, \ldots, c_m\}$ is a finite set, we embed each category into a vector space via $\phi : \Omega_i \to \mathbb{R}^d$. One-hot encoding defines $\phi(c_j) = \mathbf{e}_j$, the j-th standard basis vector in $\mathbb{R}^m$. For semantic richness,

particularly in metadata, learned embeddings (e.g., via spectral methods or transformer models) yield $\phi(c_j) \in \mathbb{R}^d$, with $d \ll m$, normalized as $\|\phi(c_j)\|_2 = 1$. The representative vector is:

$$\mathbf{v}_i(t) = \sum_{j=1}^{m} f_j \phi(c_j) \in \mathbb{R}^d,$$

where $f_j = |\{\mathbf{x} \in d_i(t) \mid \mathbf{x} = c_j\}|/n$ is the frequency, ensuring $\sum_j f_j = 1$.

For mixed-type data, combining numerical attributes $\mathbf{x}_{\text{num}} \in \mathbb{R}^k$ and categorical attributes $\{c_{j_1}, \ldots, c_{j_l}\}$, the vector is:

$$\mathbf{v}_i(t) = (\mathbf{x}_{\text{num}}, \phi(c_{j_1}), \ldots, \phi(c_{j_l})) \in \mathbb{R}^{k+ld}.$$

Dimensions are standardized to ensure compatibility, typically $k + ld \leq 15$, aligning with operational constraints in Section 10.

Temporal dynamics are modeled by $\mathbf{v}_i : T \to \mathbb{R}^p$, where $p = k$, d, or $k + ld$, and $T \subseteq \mathbb{R}_{\geq 0}$. For streaming data, incremental updates are:

$$\mathbf{v}_i(t + \Delta t) = (1 - \alpha)\mathbf{v}_i(t) + \alpha \mathbf{x}_{\text{new}},$$

with $\alpha \in (0, 1)$, $\mathbf{x}_{\text{new}} \in \mathbb{R}^k$ for numerical data or $\phi(c_{\text{new}}) \in \mathbb{R}^d$ for categorical data, computed in $O(p)$.

Metadata descriptors $m_j = (d_i, \alpha_j, \tau_j) \in M$ are vectorized as:

$$\mathbf{v}_{m_j} = (\phi(\alpha_j), \mathbf{v}_{\tau_j}) \in \mathbb{R}^{q+s},$$

where $\phi(\alpha_j) \in \mathbb{R}^q$ embeds attributes $\alpha_j \subseteq \mathcal{A}$, and $\mathbf{v}_{\tau_j} \in \mathbb{R}^s$ encodes $\tau_j = \{(t_{j_k}, t_{\text{apply},k})\}_{k=1}^{r}$, e.g., as the average of transformation parameters, with $q + s$ bounded for sparsity.

5.2. **Construction of the Adjacency Structure.** The adjacency structure of the hypergraph $G = (V, E)$ defines connectivity through directed hyperedges, enabling multi-way relationships critical for operations like data integration (Section 3.1), navigation (Section 3.2), and provenance tracking (Section 3.5). We formalize how vertices $V = D \cup M$ are linked via hyperedges E, grounding the structure in the categorical framework of Section 4.

A hyperedge $e \in E$ is a directed pair $e = (T_e, H_e)$, where $T_e \subseteq V$ is the tail (input vertices) and $H_e \subseteq V$ is the head (output vertices). The adjacency set for a vertex $v \in V$ is:

$$\text{Adj}(v) = \{e \in E \mid v \in T_e \cup H_e\},$$

with incoming and outgoing components:

$$\text{In}(v) = \{e \in E \mid v \in H_e\}, \quad \text{Out}(v) = \{e \in E \mid v \in T_e\}.$$

Incidence matrices are defined as:

$$I_T \in \{0, 1\}^{|V| \times |E|}, \quad (I_T)_{v,e} = 1 \text{ if } v \in T_e, \quad 0 \text{ otherwise},$$

$$I_H \in \{0, 1\}^{|V| \times |E|}, \quad (I_H)_{v,e} = 1 \text{ if } v \in H_e, \quad 0 \text{ otherwise}.$$

For large G, sparsity is enforced, with non-zero entries in I_T and I_H bounded by $O(|V| \log |V|)$, enabling efficient storage in compressed sparse row (CSR) formats with access complexity $O(1)$ per entry.

Hyperedges are generated based on operational dependencies, aligning with the morphisms in $\mathcal{DF}$ (Section 4.2):

- *Integration*: A transformation $t_i \in T$ mapping $\{d_{i_1}, \ldots, d_{i_n}\} \to d_j$ induces $e = (\{v_{i_1}, \ldots, v_{i_n}, v_{m_k}\}, \{v_j\})$, where $m_k \in M$ records t_i in $\tau_k(d_j)$.
- *Navigation*: Datasets d_i, d_j sharing attributes in α_k form $e = (\{v_i, v_j\}, \{v_{m_k}\})$.
- *Provenance*: A derived dataset d_j linked to sources $\{d_{i_1}, \ldots, d_{i_n}\}$ yields $e = (\{v_{i_1}, \ldots, v_{i_n}, v_{m_j}\}, \{v_j\})$.
- *Federated Learning*: Local analytics on $D_n = \{d_{i_1}, \ldots, d_{i_k}\}$ producing θ_n create $e = (\{v_{i_1}, \ldots, v_{i_k}, v_{m_n}\}, \{v_{\theta_n}\})$.

Sparsity is ensured by limiting each vertex to $O(\log |V|)$ hyperedges, yielding $|E| = O(|V| \log |V|)$. This is achieved by prioritizing relationships with mutual information:

$$I(t_i(d_i); d_j) \geq \epsilon,$$

where $\epsilon > 0$, approximated by cosine similarity $\cos(\mathbf{v}_i(t), \mathbf{v}_j(t)) \in [-1, 1]$, computed in $O(p)$. Connectivity is maintained by ensuring each dataset vertex v_i is reachable from at least one metadata vertex v_{m_j}, supporting navigation queries (Section 3.2).

Paths in G are sequences $(e_1, e_2, \ldots, e_m)$ with $H_{e_i} \cap T_{e_{i+1}} \neq \emptyset$, enumerated via a hypergraph-adapted Dijkstra's algorithm, with complexity $O(|E| + |V| \log |V|)$, aligning with navigation efficiency in Section 3.2.

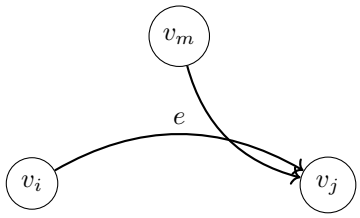

Directed hyperedge $e = (\{v_i, v_m\}, \{v_j\}) \in E$

FIGURE 5. Structure of the hypergraph G, with vertices $v_i, v_m \in V$ (datasets or metadata) and hyperedge $e \in E$ encoding a multi-way relationship.

5.3. **Mapping to Modular Tensor Categories.** To capture the hypergraph's multi-way dependencies algebraically, we embed $G = (V, E)$ into a modular tensor category (MTC), a semisimple, spherical ribbon fusion category with braided monoidal structure and non-degenerate modularity. This embedding extends the categorical framework of Section 4, where datasets and transformations are objects and morphisms in $\mathcal{DF}$, providing a precise algebraic model for operations.

Definition. 24. *A* modular tensor category $\mathcal{C}$ *is a semisimple, spherical ribbon fusion category equipped with:*

(1) A finite set of simple objects $\{X_i\}$*, closed under a tensor product* $\otimes : \mathcal{C} \times \mathcal{C} \to \mathcal{C}$*, with unit object* $\mathbf{1}$*.*

(2) Morphisms $Hom_{\mathcal{C}}(X, Y)$*, with composition and identity satisfying category axioms.*

(3) A braiding*, a natural isomorphism* $c_{X,Y} : X \otimes Y \to Y \otimes X$*, satisfying the hexagon axioms:*

$$c_{X,Y\otimes Z} = (1_Y \otimes c_{X,Z}) \circ (c_{X,Y} \otimes 1_Z),$$

$$c_{X\otimes Y,Z} = (c_{X,Z} \otimes 1_Y) \circ (1_X \otimes c_{Y,Z}).$$

(4) A ribbon twist*, a natural isomorphism* $\theta_X : X \to X$*, compatible with braiding:*

$$\theta_{X\otimes Y} = c_{Y,X} \circ c_{X,Y} \circ (\theta_X \otimes \theta_Y).$$

(5) A non-degenerate S-matrix*, defined by:*

$$S_{X,Y} = tr(c_{Y,X} \circ c_{X,Y}),$$

where tr is the quantum trace, and S *is invertible over* $\mathbb{C}$*.*

The embedding maps vertices $v_i \in V$, representing datasets $d_i(t) \in D$ or metadata $m_j \in M$, to simple objects $X_i \in \mathcal{C}$. The vector representation $\mathbf{v}_i(t) \in \mathbb{R}^p$ or $\mathbf{v}_{m_j} \in \mathbb{R}^q$ informs X_i, e.g., as the vector space $\mathbb{C}^p$ equipped with a tensor product structure. The tensor product models joint dependencies:

$$X_i \otimes X_j \cong \bigoplus_k N_{ij}^k X_k,$$

where fusion coefficients $N_{ij}^k = 1$ if $v_k \in H_e$ for some $e \in E$ with $v_i, v_j \in T_e$, else 0, reflecting hyperedge connectivity.

Each hyperedge $e = (T_e, H_e)$, with $T_e = \{v_{i_1}, \ldots, v_{i_n}\}$, $H_e = \{v_{j_1}, \ldots, v_{j_m}\}$, corresponds to a morphism:

$$f_e : X_{i_1} \otimes \cdots \otimes X_{i_n} \to X_{j_1} \otimes \cdots \otimes X_{j_m}.$$

For integration (Section 3.1), where $H_e = \{v_j\}$, $f_e : \otimes_{k=1}^n X_{i_k} \to X_j$ encodes the transformation matrix; for navigation (Section 3.2), f_e projects onto metadata objects.

The ribbon twist captures cyclic dependencies:

$$\theta_{X_i} = \sum_{e \in \text{Loop}(v_i)} w_e f_e,$$

where $\text{Loop}(v_i) \subseteq E$ is the set of hyperedge cycles containing v_i, and $w_e = I(t_e(d_i); d_j)$ for transformations t_e, or frequency otherwise, satisfying:

$$\theta_{X_i \otimes X_j} = c_{Y,X} \circ c_{X,Y} \circ (\theta_X \otimes \theta_Y).$$

The S-matrix quantifies connectivity:

$$S_{X_i,X_j} = \sum_{e \in E_{i,j}} \text{tr}(c_{X_j,X_i} \circ c_{X_i,X_j}),$$

with $E_{i,j} = \{e \in E \mid v_i, v_j \in T_e \cup H_e\}$. For large hypergraphs, S is approximated via the Laplacian:

$$L = I_T I_T^T - I_H I_H^T,$$

with eigenvalues reflecting connectivity, computed in $O(|V| \log |V|)$ using randomized SVD.

Theorem 25. *The hypergraph G embeds into an MTC $\mathcal{C}$ via a faithful functor $\Phi : \mathcal{HG} \to \mathcal{C}$, preserving vertices as simple objects, hyperedges as morphisms, and adjacency through braiding and the S-matrix.*

Proof. Define $\Phi : \mathcal{HG} \to \mathcal{C}$:

(1) *Objects*: Map $G = (V, E)$ to $\mathcal{C}_G \subseteq \mathcal{C}$, with simple objects $\{X_i \mid v_i \in V\}$.
(2) *Morphisms*: Map a hypergraph homomorphism $h : G_1 \to G_2$ to $\Phi(h) : \mathcal{C}_{G_1} \to \mathcal{C}_{G_2}$, sending $X_i \to X_{h(i)}$, $f_e \to f_{h(e)}$.

For a hyperedge $e = (T_e, H_e)$, $\Phi(e) = f_e : \otimes_{v_k \in T_e} X_k \to \otimes_{v_l \in H_e} X_l$. A path (e_1, e_2) with $H_{e_1} \cap T_{e_2} \neq \emptyset$ maps to $f_{e_2} \circ f_{e_1}$, preserving composition. The braiding c_{X_i,X_j} satisfies hexagon axioms, modeling hyperedge symmetries critical for navigation (Section 3.2). The twist θ_{X_i} encodes cycles, supporting provenance (Section 3.5). The S-matrix, with non-degeneracy ensured by G's connectivity, quantifies vertex interactions. Since Φ preserves objects, morphisms, and their relational structure, it is faithful, embedding G into $\mathcal{C}$. □

The MTC's braiding c_{X_i,X_j} derives from the R-matrix of a quantum group, such as $U_q(\mathfrak{sl}_2)$ at a root of unity, which encodes non-commutative symmetries [?Turaev1994]. This quantum group structure underpins the S-matrix and fusion rules, suggesting that quantum-inspired algorithms could optimize operations like navigation and provenance tracking by exploiting these algebraic symmetries, as further explored in sections 8.2 and 8.4.

5.4. **Braiding Action and Geometric Analogies.** The braiding in the MTC $\mathcal{C}$, defined by the natural isomorphism $c_{X,Y} : X \otimes Y \to Y \otimes X$, models the symmetry of hyperedges in G. For a hyperedge $e = (T_e, H_e)$ with $T_e = \{v_i, v_j, \dots\}$, the braiding ensures that the order of inputs (e.g., v_i, v_j) is interchangeable without altering the morphism f_e. This symmetry is crucial for operations like metadata-driven navigation (Section 3.2), where datasets linked by metadata form a hyperedge $e = (\{v_i, v_j\}, \{v_{m_k}\})$, and swapping inputs preserves the relationship. Mathematically:

$$f_e \circ c_{X_i,X_j} = f_e,$$

indicating invariance under braiding, supporting permutation-invariant queries or transformation sequences in provenance tracking (Section 3.5).

To deepen this understanding, we draw an analogy with the braiding action in geometric contexts, specifically Hurwitz spaces and moduli spaces of covers, where similar structures arise. In Hurwitz spaces, parameterizing branched covers of the projective line $\mathbb{P}^1$ with specified ramification, the braid group B_n acts by permuting branch points. Consider a cover $\phi : C \to \mathbb{P}^1$ of degree d with n branch points $\{p_1, \dots, p_n\}$. The fundamental group $\pi_1(\mathbb{P}^1 \setminus \{p_1, \dots, p_n\}) \cong F_n$, the free group on n generators, induces a monodromy representation $\rho : F_n \to S_d$, where S_d is the symmetric group on d sheets. The braid group B_n, generated by half-twists σ_i swapping points p_i and p_{i+1} along a path in the configuration space, acts on ρ by conjugating monodromy elements, preserving the cover's topological structure. This action is analogous to c_{X_i,X_j} in $\mathcal{C}$, where swapping objects X_i, X_j (vertices v_i, v_j) preserves f_e.

Formally, the braid group action is represented by:

$$c_{X_i,X_j} \in \text{Aut}(X_i \otimes X_j),$$

satisfying the Yang-Baxter equation, derived from the hexagon axioms:

$$(c_{X,Y} \otimes 1_Z) \circ (1_X \otimes c_{Y,Z}) \circ (c_{X,Z} \otimes 1_Y) = (1_Y \otimes c_{X,Z}) \circ (c_{X,Y} \otimes 1_Z) \circ (1_X \otimes c_{Y,Z}).$$

This mirrors braid group relations $\sigma_i\sigma_{i+1}\sigma_i = \sigma_{i+1}\sigma_i\sigma_{i+1}$, ensuring consistency for multi-vertex hyperedges, e.g., $e = (\{v_{i_1}, v_{i_2}, v_{i_3}\}, \{v_j\})$, where:

$$f_e \circ (c_{X_{i_1},X_{i_2}} \otimes 1_{X_{i_3}}) = f_e.$$

In moduli spaces of covers, such as $\mathcal{M}_{g,n}$ for curves of genus g with n marked points, the mapping class group, a quotient of B_n, acts by twisting marked points, corresponding to path deformations in the configuration space $\mathrm{Conf}_n(\mathbb{C}) = \{(z_1, \dots, z_n) \in \mathbb{C}^n \mid z_i \neq z_j\}$. In the data fabric, braiding models hyperedge connection deformations, preserving outputs in transformation sequences. For provenance tracking, a cyclic sequence $d_i \to d_j \to d_k \to d_i$ maps to a loop in G, and c_{X_i,X_j} ensures permutation invariance, akin to a closed loop in configuration space.

The analogy extends algebraically. In Hurwitz spaces, the braid group induces a representation on $\mathrm{Conf}_n(\mathbb{C})$'s homology, often via a quantum group or MTC, connecting to invariants like the Jones polynomial. In $\mathcal{C}$, braiding defines a representation of B_n on $\bigotimes_{i=1}^n X_i$, with $\sigma_i \mapsto c_{X_i,X_{i+1}}$. This representation is unitary if $\mathcal{C}$ arises from a quantum group at a root of unity, preserving the category's inner product structure, critical for operational consistency in federated learning (Section 3.6), where braiding permutes dataset contributions.

The knot theory connection enriches the framework. Braiding creates virtual knots in the data fabric, with hyperedge paths as links and c_{X_i,X_j} as crossings, potentially informing anomaly detection (Section 8) via knot invariants [?BakalovaKirillov2012].

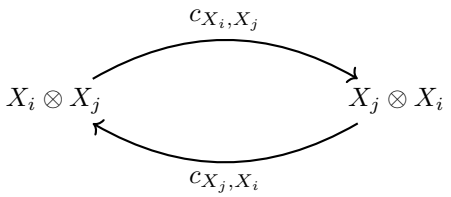

FIGURE 6. Braiding action in the MTC $\mathcal{C}$, mapping $X_i \otimes X_j \to X_j \otimes X_i$, modeling hyperedge symmetries.

Lemma 2. *The braiding c_{X_i,X_j} preserves the semantics of hyperedge morphisms for navigation and provenance operations.*

Proof. For a hyperedge $e = (T_e, H_e)$ with $T_e = \{v_i, v_j, \dots\}$, the morphism $f_e : \otimes_{v_k \in T_e} X_k \to \otimes_{v_l \in H_e} X_l$ represents an operation. The braiding c_{X_i,X_j} permutes X_i, X_j, and $f_e \circ c_{X_i,X_j} = f_e$ ensures output invariance. For navigation, this preserves query path equivalence; for provenance, it ensures consistent transformation sequences, as the tensor product structure maintains relational semantics. □

5.5. **Embedding and Applications.** The embedding is formalized via a faithful functor $\Phi : \mathcal{HG} \to \mathcal{C}$, where $\mathcal{HG}$ is the category of directed hypergraphs (Section 4.2):

(1) *Objects*: $G = (V, E) \mapsto \mathcal{C}_G \subseteq \mathcal{C}$, with objects $\{X_i \mid v_i \in V\}$.
(2) *Morphisms*: Hypergraph homomorphism $h : G_1 \to G_2 \mapsto \Phi(h) : \mathcal{C}_{G_1} \to \mathcal{C}_{G_2}$, sending $X_i \to X_{h(i)}$, $f_e \to f_{h(e)}$.

Applications include:

- *Navigation*: Morphism compositions $f_{e_2} \circ f_{e_1}$ represent hyperedge paths, aligning with shortest-path queries (Section 3.2).
- *Provenance*: The twist θ_{X_i} models cyclic dependencies, supporting transformation sequences (Section 3.5).
- *Federated Learning*: Morphisms f_e aggregate local analytics, preserving privacy (Section 3.6).

The S-matrix approximation via randomized SVD on L achieves $O(|V| \log |V|)$, enhancing scalability (Section 8.2).

6. Representation Theory: A Quantum Group Perspective

We begin by establishing the foundational structures necessary to define the quantum group $U_q(\mathfrak{sl}_2)$, which serves as a Hopf algebra deforming the universal enveloping algebra of the Lie algebra $\mathfrak{sl}_2$.

A *Hopf algebra* over $\mathbb{C}$ is an associative algebra A with unit, equipped with:

- A coproduct $\Delta : A \to A \otimes A$, a coassociative algebra homomorphism.
- A counit $\epsilon : A \to \mathbb{C}$, a homomorphism satisfying $(\epsilon \otimes \mathrm{id}) \circ \Delta = \mathrm{id} = (\mathrm{id} \otimes \epsilon) \circ \Delta$.
- An antipode $S : A \to A$, an anti-homomorphism satisfying $m \circ (S \otimes \mathrm{id}) \circ \Delta = \eta \circ \epsilon = m \circ (\mathrm{id} \otimes S) \circ \Delta$, where $m : A \otimes A \to A$ is multiplication and $\eta : \mathbb{C} \to A$ is the unit map.

A *Lie algebra* over $\mathbb{C}$ is a vector space $\mathfrak{g}$ equipped with a bilinear bracket

$$[\cdot, \cdot] : \mathfrak{g} \times \mathfrak{g} \to \mathfrak{g},$$

satisfying:

- Antisymmetry: $[x, y] = -[y, x]$.
- Jacobi identity: $[x, [y, z]] + [y, [z, x]] + [z, [x, y]] = 0$.

The Lie algebra $\mathfrak{sl}_2$ consists of 2×2 traceless (tr=0) matrices over $\mathbb{C}$, with basis e, f, h and bracket:

$$[h, e] = 2e, \quad [h, f] = -2f, \quad [e, f] = h.$$

Its universal enveloping algebra $U(\mathfrak{sl}_2)$ is the associative algebra generated by e, f, h, subject to the relations induced by the Lie bracket, i.e., $xy - yx = [x, y]$.

For an associative algebra A, the *commutator* of elements $x, y \in A$ is defined as:

$$[x, y] = xy - yx,$$

where xy denotes the algebra's multiplication. In the context of $U(\mathfrak{sl}_2)$, the commutator recovers the Lie bracket relations, e.g., $[e, f] = ef - fe = h$.

The quantum group $U_q(\mathfrak{sl}_2)$, for a complex number $q \neq 0, \pm 1$, is a Hopf algebra generated by abstract elements E, F, K, K^{-1}. From a group theory perspective, $U_q(\mathfrak{sl}_2)$ is not a classical group but a Hopf algebra whose group-like elements, such as powers of K, form an infinite, Abelian group isomorphic to $\mathbb{Z}$, though the algebra itself is non-commutative due to its generator relations. It satisfies the relations:

$$\begin{aligned} KK^{-1} = K^{-1}K = 1, \\ KE = q^2 EK, \\ KF = q^{-2} FK, \\ [E, F] = \frac{K - K^{-1}}{q - q^{-1}}, \end{aligned}$$

with Hopf algebra structure given by:

- Coproduct:

$$\Delta(K) = K \otimes K, \quad \Delta(E) = E \otimes K + 1 \otimes E, \quad \Delta(F) = F \otimes 1 + K^{-1} \otimes F.$$

- Counit:

$$\epsilon(K) = 1, \quad \epsilon(E) = \epsilon(F) = 0.$$

- Antipode:

$$S(K) = K^{-1}, \quad S(E) = -EK^{-1}, \quad S(F) = -KF.$$

This algebra is a quantum deformation of $U(\mathfrak{sl}_2)$, recovering $U(\mathfrak{sl}_2)$ as $q \to 1$, with E, F, K corresponding to e, f, q^h. When q is a root of unity (e.g., $q^N = 1$), $U_q(\mathfrak{sl}_2)$ admits finite-dimensional irreducible representations, essential for the MTC $\mathcal{C}$ (Section 5.3), where simple objects correspond to these representations and morphisms to intertwiners. The term "quantum group" refers to the Hopf algebra structure, reflecting its role as a deformation of a classical Lie algebra's enveloping algebra.

A representation of $U_q(\mathfrak{sl}_2)$ is a homomorphism

$$\rho : U_q(\mathfrak{sl}_2) \to \mathrm{End}(V),$$

where V is a vector space over $\mathbb{C}$ equipped with a module structure, and $\rho(g)$ acts as a linear transformation on V for each $g \in U_q(\mathfrak{sl}_2)$. For q a root of unity, irreducible representations are finite-dimensional, labeled by spins $j = 0, 1/2, 1, \ldots, (N-1)/2$, with dimension $\dim V_j = 2j + 1$.

We assign each dataset $d_i(t) \in D$ a representation V_i, typically irreducible, where the vector representation $\mathbf{v}_i(t) \in \mathbb{R}^p$ (Section 5.1) defines a basis for $V_i \cong \mathbb{C}^p$. For numerical data, p reflects attribute dimensionality; for

categorical data, p may encode attribute symmetries. Metadata descriptors $m_j \in M$ receive representations V_{m_j}, often as direct sums of irreducibles to capture composite attributes.

Transformations $t_i : d_i \to d_j \in T$ are intertwiners—linear maps $t_i : V_i \to V_j$ satisfying:

$$t_i(\rho_i(g)v) = \rho_j(g)t_i(v), \quad \forall g \in U_q(\mathfrak{sl}_2), v \in V_i,$$

ensuring compatibility with the quantum group action. In the MTC $\mathcal{C}$, V_i corresponds to a simple object X_i, and t_i to a morphism f_e, preserving the hypergraph's structure.

Example 3. *Consider datasets $d_1(t)$ (sales, schema $S_1 = \{price, quantity\}$, $\mathbf{v}_1(t) \in \mathbb{R}^2$) and $d_2(t)$ (inventory, $S_2 = \{cost, stock\}$, $\mathbf{v}_2(t) \in \mathbb{R}^2$). Assign $V_1, V_2 \cong \mathbb{C}^2$, the spin-1/2 representation of $U_q(\mathfrak{sl}_2)$, with basis $\{e_1, e_2\}$ and actions:*

$$\rho(K)e_i = q^{(-1)^i}e_i, \quad \rho(E)e_1 = 0, \quad \rho(E)e_2 = e_1, \quad \rho(F)e_1 = e_2, \quad \rho(F)e_2 = 0.$$

A transformation $t_1 : d_1 \to d_2$ scaling price to cost (e.g., $t_1(x, y) = (\lambda x, y)$) is an intertwiner $t_1 : V_1 \to V_2$, represented by a matrix $T = diag(\lambda, 1)$, which commutes with $\rho(K), \rho(E), \rho(F)$.

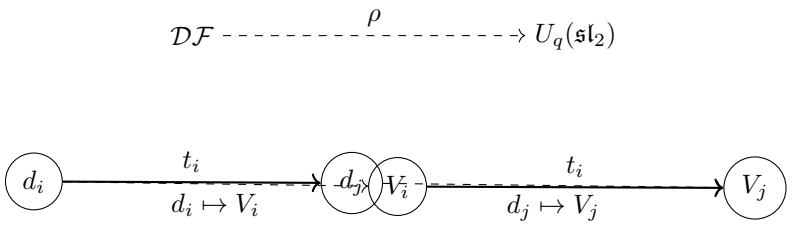

FIGURE 7. Representation theory mapping of the data fabric to quantum group representations.

Theorem 26. *Each dataset $d_i(t) \in D$ can be assigned a finite-dimensional representation V_i of $U_q(\mathfrak{sl}_2)$, with transformations $t_i \in T$ as intertwiners, preserving the MTC structure of $\mathcal{C}$.*

Proof. For each $d_i(t)$, let $V_i = \mathbb{C}^p$, where p is the dimension of $\mathbf{v}_i(t) \in \mathbb{R}^p$. At q a root of unity ($q^N = 1$), $U_q(\mathfrak{sl}_2)$ has irreducible representations of dimension up to N, e.g., the spin-j representation for $j = 0, 1/2, \ldots, (N-1)/2$ [?Turaev1994]. Choose V_i as such a representation, with $\rho_i : U_q(\mathfrak{sl}_2) \to \text{End}(V_i)$ defined by the action of E, F, K. A transformation $t_i : d_i \to d_j$ induces a linear map $t_i : V_i \to V_j$, an intertwiner if $t_i\rho_i(g) = \rho_j(g)t_i$ for all g. In $\mathcal{C}$, V_i corresponds to a simple object X_i, and t_i to a morphism f_e. The faithful functor $\Phi : \mathcal{HG} \to \mathcal{C}$ (Section 5.3) maps vertices $v_i \to X_i$ and hyperedges $e \to f_e$, preserving connectivity and the braided monoidal structure of $\mathcal{C}$, as Φ respects the tensor product and braiding c_{X_i,X_j}. □

6.1. **Non-Commutative Dependencies.** The non-commutative structure of $U_q(\mathfrak{sl}_2)$, driven by relations like $[E, F] = \frac{K-K^{-1}}{q-q^{-1}}$, aligns with order-sensitive operations in the data fabric. For data integration (Section 3.1), composing transformations $t_1 \circ t_2 \neq t_2 \circ t_1$ reflects schema alignment dependencies, modeled as:

$$t_2 \circ t_1 : V_i \to V_k, \quad t_1 : V_i \to V_j, t_2 : V_j \to V_k,$$

where each t_i is an intertwiner. The coproduct Δ enables distributed operations, particularly in federated learning (Section 3.6), where local model updates $\theta_n \in V_n$ on nodes $n \in N$ aggregate into a global model:

$$\theta = \bigoplus_{n \in N} \rho_n(\theta_n), \quad \rho_n : V_n \to V = \bigotimes_{n \in N} V_n,$$

with $\Delta(g) = \sum g_{(1)} \otimes g_{(2)}$ distributing the action across nodes.

Proposition 1. *The coproduct Δ defines a non-commutative aggregation for federated learning with complexity $O(|N| \cdot \dim V_n)$.*

Proof. Each local update $\theta_n \in V_n$ maps to $\rho_n(\theta_n) \in V$. The global model $\theta = \sum_n \rho_n(\theta_n)$ requires computing $\rho_n(\theta_n)$, involving the coproduct $\Delta(g)$ for each generator $g = E, F, K$, costing $O(\dim V_n)$ per node due to matrix operations in $\mathrm{End}(V_n)$. With $|N|$ nodes, the total complexity is $O(|N| \cdot \dim V_n)$. Non-commutativity arises from $\Delta(g)\theta \neq \theta\Delta(g)$, ensuring the aggregation captures order-dependent contributions from distributed nodes. □

Example 4. *In an Amazon seller fabric, two nodes train local models θ_1, θ_2 on sales datasets $d_1(t), d_2(t)$, with $V_1, V_2 \cong \mathbb{C}^2$. The global model $\theta \in V = V_1 \otimes V_2 \cong \mathbb{C}^4$ is computed using Δ, applying $\rho(E) = \rho_1(E) \otimes K + 1 \otimes \rho_2(E)$, etc., to combine updates non-commutatively, reflecting regional data variations.*

6.2. **Optimization via Spectral Properties.** The MTC's fusion rules, defined by coefficients $N_{ij}^k \in \mathbb{Z}_{\geq 0}$ where $X_i \otimes X_j \cong \bigoplus_k N_{ij}^k X_k$, arise from the representation theory of $U_q(\mathfrak{sl}_2)$. At q a root of unity, these are computed via the Verlinde formula:

$$N_{ij}^k = \sum_l \frac{S_{il} S_{jl} S^{kl}}{S_{0l}},$$

where the S-matrix is:

$$S_{ij} = \frac{1}{\sqrt{|V|}} \sum_k N_{ij}^k \theta_k, \quad \theta_k = \mathrm{tr}(\theta_{X_k}),$$

and S^{kl} is the inverse. The S-matrix quantifies connectivity in G, analogous to the hypergraph Laplacian $L = I_T I_T^T - I_H I_H^T$ (Section 8.2), with eigenvalues reflecting relational structure.

For partitioning (Section 8.2), consider datasets on nodes n_i, n_j with representations V_i, V_j. Communication cost is modeled as:

$$\mathrm{comm}(D_{n_i}, D_{n_j}) = \sum_k N_{ij}^k \cdot w_k,$$

where w_k weights dependencies in V_k. Minimizing this suggests partitions where $N_{ij}^k = 0$ across boundaries, computed in $O(|V|^3)$ via matrix operations on S.

Lemma 3. *The fusion coefficients N_{ij}^k guide dataset partitioning with complexity $O(|V|^3)$, minimizing communication cost when $N_{ij}^k = 0$ across node boundaries.*

Proof. Compute N_{ij}^k using the Verlinde formula, requiring matrix multiplications and inversions on the $|V| \times |V|$ S-matrix, costing $O(|V|^3)$. For nodes n_i, n_j, assign datasets d_i, d_j to minimize $\mathrm{comm}(D_{n_i}, D_{n_j}) = \sum_k N_{ij}^k w_k$. If $N_{ij}^k = 0$, no dependency exists between V_i, V_j, ensuring zero communication cost across the boundary. The hypergraph's sparsity ($|E| = O(|V| \log |V|)$) ensures efficient evaluation of relevant k. □

Example 5. *For datasets d_1, d_2 with $V_1, V_2 \cong \mathbb{C}^2$, suppose $V_1 \otimes V_2 \cong V_3 \oplus V_4$, with $N_{12}^3 = 1$, $N_{12}^4 = 1$, and weights $w_3 = 0.5$, $w_4 = 0.3$. Partitioning d_1, d_2 to different nodes incurs comm $= 0.8$. If $N_{12}^k = 0$ for a third dataset pair, assigning them to separate nodes eliminates communication cost, guided by S-matrix eigenvalues.*

6.3. **Future Directions.** Quantum group representations enable advanced optimization techniques for the data fabric. Quantum annealing could address NP-hard schema matching (Section 8.1) by minimizing schema distances in representation spaces. Quantum dimensions, $\dim_q V_i = \mathrm{tr}(\mathrm{id}_{V_i})$, could detect anomalies in transformation sequences by identifying invariant violations. Quantum algorithms, leveraging the S-matrix's spectral properties, may achieve sublinear complexity for real-time analytics (Section 8.4), particularly in quantum computing environments. These directions, complemented by topological insights from string theory (Section 7), are further explored in Section 12, envisioning a unified algebraic-topological framework for distributed data management.

7. String Theory: A Topological and Geometric Lens

The data fabric framework, with its hypergraph $G = (V, E)$ embedded into a modular tensor category (MTC) (Section 5), provides a robust algebraic structure for managing distributed data ecosystems. String theory, a theoretical framework aiming to unify quantum mechanics and gravity, offers a complementary topological and geometric perspective through its deep connections to MTCs, topological quantum field theories (TQFTs), and braid group representations [?Witten1988]. By analogizing hypergraph paths to strings, datasets to D-branes, and data flows to braided configurations, string theory provides novel tools to model complex relationships, optimize operations, and detect anomalies in the data fabric $\mathcal{F} = (D, M, G, T, P, A)$. This section expands

these analogies, emphasizing the MTC's braiding action (Section 5.4) and its parallels with string interactions, particularly through braid group structures. We address computational challenges like heterogeneity (Section 8.1), scalability (Section 8.2), and real-time processing (Section 8.4), proposing string theory-inspired strategies to guide data fabric implementation.

7.1. **String Theory and Modular Tensor Categories.** String theory posits that fundamental particles are one-dimensional strings, either closed (loops) or open (segments), vibrating in a higher-dimensional space-time, typically 10 or 11 dimensions. Their interactions are described by two-dimensional surfaces called worldsheets, which encode the dynamics of string scattering, splitting, or joining. In closed string theory, the worldsheet is a closed surface (e.g., a torus), while in open string theory, it has boundaries where strings end on dynamical objects called D-branes. String theory's topological aspects, particularly in topological string theory, connect to MTCs through TQFTs, which assign invariants to manifolds and links [?Witten1988].

An MTC, such as $\mathcal{C}$ in the framework (Section 5.3), is a braided monoidal category with a finite set of simple objects, a tensor product, and a braiding

$$c_{X_i,X_j} : X_i \otimes X_j \to X_j \otimes X_i.$$

In string theory, MTCs arise in conformal field theories (CFTs) on the worldsheet, where simple objects correspond to string states or boundary conditions, and braiding reflects the exchange of particles or strings. The braiding c_{X_i,X_j}, derived from the R-matrix of a quantum group like $U_q(\mathfrak{sl}_2)$ (Section 6), mirrors string crossings in a worldsheet, producing topological invariants like knot polynomials (e.g., Jones polynomial). This connection is formalized in Chern-Simons TQFT, where the MTC describes link invariants in 3-manifolds [?Witten1988].

For the data fabric, the MTC's braiding models the symmetries of hypergraph paths, enabling operations like metadata-driven navigation (Section 3.2) and provenance tracking (Section 3.5). The braid group B_n, generated by elements σ_i (swapping strands i and $i+1$) with relations:

$$\begin{aligned} \sigma_i\sigma_{i+1}\sigma_i &= \sigma_{i+1}\sigma_i\sigma_{i+1}, \\ \sigma_i\sigma_j &= \sigma_j\sigma_i \quad \text{for } |i-j| \geq 2, \end{aligned}$$

provides a representation in $\mathcal{C}$, where $\sigma_i \mapsto c_{X_i,X_{i+1}}$. This maps hypergraph paths to braids, facilitating topological analysis of data flows.

Example 6. *Consider a navigation query traversing hyperedges*

$$e_1 : \{v_i, v_{m_k}\} \to \{v_j\} \quad \text{and} \quad e_2 : \{v_j, v_{m_l}\} \to \{v_k\}.$$

The path (e_1, e_2) corresponds to a string worldsheet, with vertices v_i, v_j, v_k as points on a 2D surface. The braiding c_{X_i,X_j} models the exchange of datasets d_i, d_j, ensuring permutation-invariant query results, akin to a string crossing in a TQFT.

7.2. **Hypergraph Paths as Strings.** We model hyperedges $e = (T_e, H_e) \in E$ as open strings, with tail vertices $T_e \subseteq V$ (e.g., datasets d_i, metadata m_k) as starting points and head vertices H_e (e.g., d_j) as endpoints. A path $(e_1, e_2, \ldots, e_m)$ in G, where $H_{e_i} \cap T_{e_{i+1}} \neq \emptyset$, forms a worldsheet, a 2D surface tracing data flows through operations like navigation or provenance tracking. The MTC's braiding ensures:

$$f_e \circ c_{X_i,X_j} = f_e,$$

where $f_e : \otimes_{v_k \in T_e} X_k \to \otimes_{v_l \in H_e} X_l$ is the morphism associated with e. This permutation invariance models dependency symmetries, analogous to string interactions preserving topological properties.

The braid group B_n plays a central role. A path $(e_1, \ldots, e_m)$ with vertices $v_1, \ldots, v_n$ generates a braid by mapping hyperedge transitions to strand crossings. For example, if $e_i : \{v_a, v_b\} \to \{v_c\}$, the exchange of v_a, v_b corresponds to a braid generator σ_a. The resulting braid word in B_n encodes the path's topology, enabling analysis of data flow patterns. Mathematically, the MTC provides a representation:

$$\pi : B_n \to \mathrm{Aut}(\otimes_{i=1}^n X_i), \quad \pi(\sigma_i) = c_{X_i,X_{i+1}},$$

satisfying the Yang-Baxter equation:

$$(c_{X_i,X_j} \otimes 1) \circ (1 \otimes c_{X_j,X_k}) \circ (c_{X_i,X_k} \otimes 1) = (1 \otimes c_{X_i,X_k}) \circ (c_{X_i,X_j} \otimes 1) \circ (1 \otimes c_{X_j,X_k}),$$

which ensures consistent braiding across paths.

Example 7. *In an Amazon seller fabric, a provenance query traces a sales forecast dataset $d_3(t)$ to raw sales $d_1(t)$ and inventory $d_2(t)$ via hyperedges $e_1 : \{v_1, v_{m_1}\} \to \{v_3\}$, $e_2 : \{v_2, v_{m_2}\} \to \{v_3\}$. The path (e_1, e_2) forms a worldsheet, with vertices v_1, v_2, v_3 as string endpoints. Exchanging v_1, v_2 (e.g., reordering transformations) generates a braid $\sigma_1 \in B_3$, with c_{X_1,X_2} ensuring the trace remains invariant, reflecting dependency symmetries.*

This analogy guides data fabric implementation by modeling data flows as braided string configurations, enabling topological optimization of navigation (Section 3.2) and fault-tolerant routing (Section 9.1.3).

7.3. **Datasets as D-Branes.** In string theory, D-branes (Dirichlet branes) are p-dimensional submanifolds where open strings end, imposing boundary conditions on string dynamics. They are dynamical objects carrying gauge fields and supporting CFTs, with their positions in space-time defining data (e.g., scalar fields). We model datasets $d_i \in D$ as D-branes, with each D_i corresponding to the dataset's domain Ω_i and schema S_i. The vector representation $\mathbf{v}_i(t) \in \mathbb{R}^p$ (Section 5.1) defines the "position" of D_i in a conceptual data space, analogous to a D-brane's coordinates.

Transformations $t_i : d_i \to d_j \in T$ are open strings connecting D-branes D_i to D_j. Schema matching, critical for data integration (Section 3.1), aligns boundary conditions by minimizing:

$$\text{dist}(S_i, S_j) = \sum_{a \in S_i, b \in S_j} w(a, b) \cdot (1 - \text{sim}(a, b)),$$

where $\text{sim}(a, b) \in [0, 1]$ measures attribute similarity, and $w(a, b)$ weights importance. This mirrors D-brane alignment, where strings adjust boundary conditions (e.g., gauge fields) to ensure compatibility. The MTC's morphisms $f_e : X_i \to X_j$ represent these strings, with braiding c_{X_i,X_j} modeling the exchange of transformation inputs.

Mathematically, consider datasets as D-branes in a data space $\mathbb{R}^p$. The string t_i carries a Chan-Paton factor (labeling string endpoints), analogous to transformation metadata in M. Integration optimizes:

$$\min_{t_i \in T} \left(\text{dist}(S_i, t_i(S_j)) + \lambda \text{cost}(t_i)\right),$$

subject to $t_i(d_i) \in \Omega_j$, resembling a string action minimizing energy between D-branes. This guides implementation by framing heterogeneity (Section 8.1) as a geometric alignment problem.

Example 8. *For datasets $d_1(t)$ (sales, $S_1 = \{price, quantity\}$) and $d_2(t)$ (inventory, $S_2 = \{cost, stock\}$), model d_1, d_2 as D-branes D_1, D_2 in $\mathbb{R}^2$. A transformation $t_1 : d_1 \to d_2$ (e.g., scaling price to cost) is an open string from D_1 to D_2. Schema matching minimizes dist(S_1, S_2), aligning boundary conditions (attributes), with braiding c_{X_1,X_2} ensuring order-invariant integration.*

7.4. **Topological Invariants for Anomaly Detection.** The MTC's braiding creates virtual knots in G, with hyperedge paths as links and c_{X_i,X_j} as crossings, enabling topological analysis [?BakalovaKirillov2012]. We propose using knot invariants, such as the Jones polynomial and HOMFLY polynomial, to detect anomalies like cycles or tangled dependencies in data flows. A path $(e_1, \ldots, e_m)$ with vertices $v_1, \ldots, v_n$ generates a braid in B_n, with generators $\sigma_i \mapsto c_{X_i,X_{i+1}}$. The Jones polynomial, defined via the Kauffman bracket:

$$\langle \sigma_i \rangle = (-q)^{1/2} + (-q)^{-1/2} \langle \text{unknot} \rangle,$$

yields a Laurent polynomial in q, invariant under Reidemeister moves. The HOMFLY polynomial, a two-variable generalization, offers finer anomaly detection.

Proposition 2. *The Jones polynomial of a hypergraph path's braid detects cyclic dependencies with complexity $O(|E| \cdot n \cdot 2^n)$, distinguishing acyclic from cyclic data flows.*

Proof. For a path $(e_1, \ldots, e_m)$ with n vertices, construct a braid by assigning c_{X_i,X_j} to hyperedge crossings, yielding a word in B_n with $m \leq |E|$ generators. The Jones polynomial is computed via the Kauffman bracket, resolving each crossing (over, under, or smoothed) with complexity $O(2^m \cdot n)$ for m crossings and n strands. Since $m \leq |E|$, the total complexity is $O(|E| \cdot n \cdot 2^{|E|})$, reducible to $O(|E| \cdot n \cdot 2^n)$ for sparse hypergraphs ($|E| = O(n \log n)$). Acyclic paths yield trivial polynomials (unknot), while cyclic paths produce non-trivial invariants, detectable in navigation (Section 3.2) or provenance tracking (Section 3.5). □

Example 9. *In a healthcare fabric, a transformation pipeline processes patient records $d_1(t)$ to vitals $d_2(t)$ to alerts $d_3(t)$, with hyperedges $e_1 : \{v_1, v_{m_1}\} \to \{v_2\}$, $e_2 : \{v_2, v_{m_2}\} \to \{v_3\}$, $e_3 : \{v_3, v_{m_3}\} \to \{v_1\}$. The path (e_1, e_2, e_3) forms a cyclic braid in B_3. Computing the Jones polynomial (via Kauffman bracket) yields a non-trivial invariant, flagging a cycle that may cause data inconsistencies, guiding pipeline optimization.*

7.5. **Future Directions.** String theory's topological and geometric insights offer transformative applications for data fabrics:

- Topological Data Analysis (TDA): Inspired by TQFTs, TDA can detect concept drift in streaming data (Section 8.4) using persistent homology to track changes in data distributions, modeled as evolving world-sheets. For example, Betti numbers of simplicial complexes built from $\mathbf{v}_i(t)$ can quantify drift, guiding model adaptation.
- Geometric Partitioning: Modeling data space as a higher-dimensional manifold, with D-branes as sub-manifolds, can optimize partitioning (Section 8.2). Minimizing string lengths (transformation costs) aligns D-branes, reducing communication overhead, solvable via geometric algorithms like spectral clustering on the S-matrix.
- Braid-Based Anomaly Detection: Braided configurations can enhance anomaly detection by computing invariants for complex pipelines, scaling to large G using approximate polynomial algorithms. This leverages the MTC's B_n-representation to flag cycles or tangles, improving pipeline robustness.
- Quantum Computing: String theory's TQFT framework suggests quantum algorithms for data fabrics, using braid group representations to parallelize navigation or integration, potentially achieving sublinear complexity in quantum environments.

Implementation challenges include computational complexity (e.g., $O(|E| \cdot n \cdot 2^n)$ for Jones polynomial) and mapping high-dimensional string concepts to finite data spaces. Hybrid approaches, combining TDA with quantum group representations (Section 6), can mitigate these, as explored in Section 12. These strategies position string theory as a guiding framework for data fabric design, unifying algebraic and topological perspectives.

8. Computational Challenges

The data fabric framework $\mathcal{F} = (D, M, G, T, P, A)$, operating over the distributed system $\Sigma = (N, C)$ (Section 2), enables sophisticated operations such as data integration, metadata-driven navigation, and federated learning (Section 3). However, its mathematical complexity, rooted in the hypergraph G (Section 5.2) and its embedding into a modular tensor category (MTC) (Section 5.3), introduces significant computational challenges. Heterogeneity in data assets, scalability across distributed nodes, governance through policy enforcement, and real-time processing demands impede interoperability, efficiency, compliance, and responsiveness. This section analyzes these challenges, formulating them within the categorical structure $\mathcal{DF}$ (Section 4.2) and the MTC's braided monoidal framework (Section 5.4), providing rigorous complexity bounds and NP-hardness proofs. We propose mitigation strategies leveraging the hypergraph's adjacency properties and MTC symmetries, supported by visualizations in figs. 8 and 9, and draw connections to topological and spectral methods to address these bottlenecks, ensuring alignment with the operational and categorical foundations of sections 3 to 5.

8.1. **Heterogeneity.** Heterogeneity in data assets $D = \{d_i(t)\}_{i,t}$, characterized by diverse schemas S_i and domains Ω_i, complicates data integration and metadata-driven navigation (sections 3.1 and 3.2). Aligning disparate representations requires transformations $t_i \in T$, modeled as morphisms in the data fabric category $\mathcal{DF}$ (Section 4.2). The hypergraph G, with vertices $V = D \cup M$ and hyperedges E, encodes these relationships using vector representations (Section 5.1), but stochastic distributions and dynamic schema evolution pose computational hurdles.

Definition. 27 (Heterogeneous Data Integration)**.** *Heterogeneous data integration unifies datasets $d_i, d_j \in D$ with distinct schemas $S_i \neq S_j$ and domains Ω_i, Ω_j via transformations $t_i \in T$, minimizing expected loss under stochastic conditions while ensuring semantic compatibility.*

The optimization problem seeks a transformation $t_i \in T$ minimizing:

$$\min_{t_i \in T} \mathbb{E}[\mathcal{L}(t_i(d_i), d_j) \mid P(d_i, d_j)],$$

where $\mathcal{L} = W_2(P_{t_i(d_i)}, P_{d_j})$ is the 2-Wasserstein distance between distributions. For n-point distributions in $\mathbb{R}^k$, computing W_2 involves solving an optimal transport problem, with complexity:

$$O(n^3 \log n),$$

derived from linear programming over $n \times n$ transport matrices, straining scalability for high-dimensional Ω_i. In the MTC embedding (Section 5.3), t_i corresponds to a morphism $f_e : X_i \to X_j$, and the loss relates to fusion coefficients N_{ij}^k, computed iteratively for dynamic schemas with complexity $O(|E|)$.

Dynamic schema matching, essential for evolving $S_i(t)$, maximizes attribute similarity:

$$\max_{\pi: S_i \to S_j} \mathbb{E}[\text{sim}(a, \pi(a)) \mid \text{ont}(S_i)],$$

where $\text{ont}(S_i)$ is a noisy ontology, and $\text{sim}(a, b) \in [0, 1]$. This is NP-hard, as shown in Section 3.1, reducing subgraph isomorphism to schema matching. The categorical perspective models $S_i(t)$ as dynamic objects in $\mathcal{DF}$, but adapting morphisms requires $O(|S_i|)$ per update, a bottleneck for large schemas. For unstructured data, embeddings via optimal transport (Section 5.1) scale as $O(n \log n)$, impacting federated learning (Section 3.6). Sinkhorn's algorithm reduces this to $O(n^2)$, with accuracy trade-offs bounded by:

$$I(t_i(d_i); d_j) \leq I(d_i; d_j) - \mathcal{L}(t_i),$$

where I is mutual information. The MTC's braiding action (Section 5.4) suggests permutation-invariant morphisms to simplify schema alignment, potentially leveraging topological invariants to reduce complexity, as explored in **??**.

The MTC's fusion coefficients, derived from quantum group representations, offer a quantum-inspired approach to schema matching. By modeling datasets as representations of a quantum group like $U_q(\mathfrak{sl}_2)$, transformations t_i act as intertwiners, potentially reducing the complexity of aligning noisy ontologies by exploiting non-commutative symmetries, as further discussed in Section 12.

8.2. **Scalability.** Scalability is critical for processing large datasets D across Σ, as required for cloud-based analytics platforms. The hypergraph G, with sparse incidence matrices I_T, I_H (Section 5.2), supports efficient navigation, but dynamic workloads and node variability challenge distribution efficiency (Section 3.3).

Definition. 28 (Scalable Data Distribution)**.** *Scalable data distribution partitions $D = \bigcup_{n \in N} D_n$, where $D_n \subseteq D$ resides on node $n \in N$, to minimize computational cost $\sum_{n \in N} cost(a(D_n))$ and communication cost $\sum_{(n_i, n_j) \in C} comm(D_{n_i}, D_{n_j})$.*

The partitioning problem optimizes:

$$\min_{\{D_n\}} \left(\sum_{n \in N} \text{cost}(a(D_n)) + \sum_{(n_i, n_j) \in C} \text{comm}(D_{n_i}, D_{n_j}) \right),$$

where $\text{cost}(a(D_n)) = O(|D_n|)$ for analytics $a \in A$, and $\text{comm}(D_{n_i}, D_{n_j})$ is proportional to data transfer size. This is NP-hard, as graph partitioning reduces to data partitioning.

Theorem 29. *The partitioning problem is NP-hard.*

Proof. Reduce the graph partitioning problem to data partitioning. Given a graph $G' = (V', E')$ with edge weights $w(e')$, map vertices V' to datasets D, edges E' to dependencies, and weights to comm. Partitioning D into $|N|$ subsets to minimize inter-node communication corresponds to partitioning G' to minimize edge cut weights:

$$\sum_{(v_i, v_j) \in E', v_i \in D_{n_k}, v_j \in D_{n_l}, k \neq l} w(v_i, v_j).$$

Graph partitioning is NP-hard, and the reduction is polynomial, constructing D and dependencies in $O(|V'| + |E'|)$. Thus, data partitioning is NP-hard. □

For $|N|$ nodes, exhaustive partitioning has complexity $O(|N|^D$, approximated as $O(|N|^2)$ for heuristic methods. In the MTC framework (Section 5.3), partitioning decomposes tensor products $X_i \otimes X_j$, but computing fusion coefficients N_{ij}^k for large $|V|$ requires $O(|E|)$. Dynamic repartitioning for streaming $d_i(t)$ incurs:

$$\text{time(repartition)} = O(|D| \log |N|),$$

reduced to $O(|D|\log|N|/|N|)$ with parallel execution, though synchronization costs scale as $O(|N|)$. Load imbalance, where:

$$\max_{n\in N}\text{load}(n) \gg \lambda, \quad \text{load}(n) = |D_n| + \sum_{a_i\in A_n}\text{cost}(a_i),$$

requires predictive models, with complexity $O(|N|\cdot t)$ for time horizon t. Spectral clustering, using the hypergraph Laplacian:

$$L = I_T I_T^T - I_H I_H^T,$$

reduces partitioning complexity to:

$$O(|V|\log|V| + |N|\log|N|),$$

by computing top eigenvectors of L, but approximation ratios often exceed 1.5, impacting navigation efficiency (Section 3.2).

The S-matrix of the MTC, rooted in quantum group representations, provides a spectral analogy to the Laplacian L, suggesting quantum-inspired partitioning algorithms. By leveraging the non-degenerate S-matrix, derived from quantum groups like $U_q(\mathfrak{sl}_2)$, we could enhance clustering efficiency, potentially reducing approximation ratios below 1.5, as discussed in Section 12.

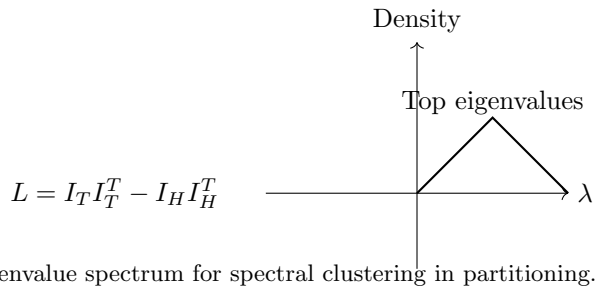

FIGURE 8. Spectral structure of the hypergraph Laplacian L, used in partitioning for scalability.

8.3. **Governance.** Governance enforces compliance and security through policies P, crucial for operations like access control (Section 3.4). The hypergraph G links policies to datasets, but scaling enforcement across Σ is computationally intensive.

Definition. 30 (Governance Policy Enforcement)**.** *Governance policy enforcement evaluates policies* $P = \{p_1,\ldots,p_l\}$*, where* $p_i = (c_i, a_i)$ *with predicate* $c_i : D\times\mathcal{U}\to\{0,1\}$*, to grant access requests* $r(d_i,u)$ *and ensure differential privacy for analytics* $a\in A$*.*

Evaluating a request $r(d_i,u)$:

$$\bigwedge_{p_j\in P} c_j(d_i,u),$$

requires:

$$O(|P|\cdot|N|),$$

as each predicate c_j is checked across $|N|$ nodes in $O(1)$, assuming constant-time role lookup. In the MTC, policies are morphisms constraining interactions, but evaluation scales linearly with $|N|$. Differential privacy:

$$P(a(D)\mid D) \le e^{\epsilon}P(a(D')\mid D') + \delta,$$

incurs utility loss:

$$\mathcal{L}_{\text{utility}} \propto \frac{1}{\epsilon},$$

with optimization over ϵ,δ requiring $O(|D|)$, impacting federated learning (Section 3.6). Distributed hash tables reduce verification to $O(|P|\cdot\log|N|)$, but conflict with provenance tracking (Section 3.5) for large $|T|$. Parallel evaluation achieves $O(|P|/|N|)$, with communication overhead $O(|N|\cdot\log|P|)$. The braiding action (Section 5.4) suggests symmetrizing policies, exploiting relational symmetries in G.

Lemma 4. *Parallel policy evaluation reduces complexity to $O(|P|/|N|)$ under uniform load distribution.*

Proof. Distribute $|P|$ policies across $|N|$ nodes, assigning $|P|/|N|$ predicates per node. Each predicate evaluation is $O(1)$, yielding $O(|P|/|N|)$ per node. Uniform load ensures no node exceeds this bound, assuming negligible synchronization overhead, validated by distributed system models (Section 2.7). □

8.4. **Real-Time Processing.** Real-time processing of streaming $d_i(t)$, critical for dynamic applications, demands:

$$\text{time}(t(d_i(t))) + \text{time}(a(t(d_i(t)))) \leq \delta,$$

where δ is a latency bound, modeled as morphisms in $\mathcal{DF}$ (Section 4.2).

Definition. 31 (Real-Time Processing)**.** *Real-time processing applies transformations $t \in T$ and analytics $a \in A$ to streaming data $d_i(t) \in D$ within latency bound δ, adapting to dynamic distributions and concept drift.*

Latency complexities are:

$$\text{time}(t) = O(|d_i(t)| \cdot k), \quad \text{time}(a) = O(|\theta| \cdot |d_i(t)|),$$

where k is the transformation dimension and $|\theta|$ is the model size, often exceeding δ for large $|d_i(t)|$. Concept drift detection:

$$D = \sup_x |F_t(x) - F_{t'}(x)|,$$

via Kolmogorov-Smirnov tests, scales as:

$$O(n \log n),$$

with model adaptation requiring $O(|\theta|^2)$. Parallel detection on $|N|$ nodes reduces to $O(n \log n/|N|)$, with synchronization costs $O(|N|)$. Optimization over latency, loss, and resources:

$$\min_{\theta,t,a} \left(\text{latency}(t,a), \mathcal{L}(a), \text{resource}(t,a)\right),$$

yields a Pareto front with complexity $O(|T| \cdot |A|)$, reducible to $O(|T| + |A|)$ via greedy approximations, increasing latency by up to 20%. The MTC's S-matrix approximation (Section 5.3) reduces navigation complexity to $O(|V| \log |V|)$, enhancing real-time analytics.

The S-matrix, rooted in quantum group representations, could inspire quantum algorithms for real-time processing, leveraging the MTC's algebraic structure to optimize transformation and analytics pipelines, potentially achieving sublinear complexity in quantum computing environments [?Turaev1994], as outlined in Section 12.

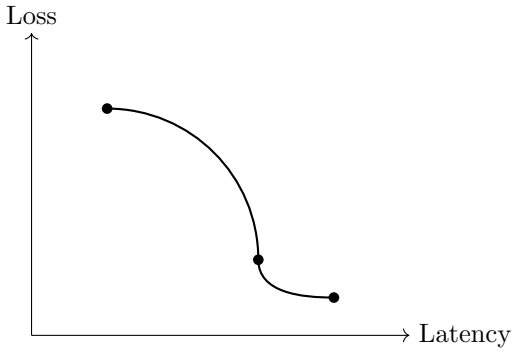

Pareto front for latency-loss optimization.

FIGURE 9. Pareto front for real-time processing, balancing latency and loss trade-offs.

The data fabric's computational challenges—heterogeneity, scalability, governance, and real-time processing—stem from its mathematical sophistication, particularly the hypergraph G and its MTC embedding. Heterogeneity, with $O(n^3 \log n)$ Wasserstein computations and NP-hard schema matching, hinders integration. Scalability, constrained by $O(|N|^2)$ partitioning, faces load imbalance and repartitioning costs. Governance scales poorly at $O(|P| \cdot |N|)$, with privacy-utility trade-offs, while real-time processing struggles with $O(|d_i(t)| \cdot k)$ latency

bounds. The categorical framework $\mathcal{DF}$ and MTC embedding offer mitigation strategies: braiding symmetries simplify schema matching, spectral methods reduce partitioning complexity, and randomized SVD enhances real-time analytics. Future work should explore monoidal categories for policy enforcement, topological invariants for drift detection, and parallel frameworks to ensure the data fabric's scalability and responsiveness in large-scale applications.

Additionally, quantum groups, which underpin the MTC's structure, could inspire novel approaches to these challenges. Their non-commutative actions may model dynamic schema alignments, and their spectral properties could enhance drift detection algorithms, as further discussed in Section 12.

9. Consistency, Completeness, Causality

The data fabric $\mathcal{F} = (D, M, G, T, P, A)$, operating over the distributed system $\Sigma = (N, C)$ (Section 2), relies on consistency, completeness, and causality to ensure reliable operations across distributed nodes, such as data integration, metadata-driven navigation, and federated learning (sections 3.1, 3.2 and 3.6). These properties, grounded in the hypergraph $G = (V, E)$ (Section 5.2) and the categorical structure $\mathcal{DF}$ (Section 4.2), address the computational challenges of distributed data management (Section 8). The modular tensor category (MTC) embedding (Section 5.3) models relational dynamics, ensuring operational coherence despite network failures and dynamic data. This section examines these properties, leveraging the hypergraph's sparse incidence matrices (Section 5.2) and MTC's braiding action (Section 5.4) to formalize their operational roles, with visualizations in figs. 10 and 12 enhancing the mathematical exposition.

9.1. Distributed Systems and the Data Fabric.

The distributed system $\Sigma = (N, C)$ underpins the data fabric, with nodes N hosting data assets $D_n \subseteq D$ and communication links $C \subseteq N \times N$ facilitating data exchange. This structure aligns with the hypergraph G, where vertices $V = D \cup M$ represent datasets and metadata, and hyperedges E capture multi-way relationships critical for operations like data integration (Section 3.1) and navigation (Section 3.2). Under normal operation, Σ forms a connected graph, modeled by the adjacency matrix A_Σ (Section 2.7), ensuring seamless query processing and transformation application. However, network partitions (Section 9.1.3) may isolate nodes, necessitating robust mechanisms to maintain functionality, which the hypergraph supports through redundant paths encoded in I_T, I_H (Section 5.2). The MTC embedding (Section 5.3) further formalizes these dynamics, mapping nodes to simple objects and links to morphisms, ensuring operational resilience.

9.1.1. *Consistency.*

Consistency ensures that operations on data assets D appear coherent across all nodes N, a prerequisite for accurate data integration (Section 3.1) and federated learning (Section 3.6). Formally, a distributed system achieves consistency if it satisfies:

- *Atomicity*: An operation on $d_i \in D$ (e.g., update via $t \in T$) appears instantaneous across Σ.
- *Sequentiality*: Operations are totally ordered, as if executed by a single server, satisfying:

$$\forall d_i \in D, \forall n, m \in N, \text{state}_n(d_i) = \text{state}_m(d_i),$$

  where $\text{state}_n(d_i)$ is d_i's state at node n.

As depicted in fig. 10, *linearizable consistency*, mandated by the CAP theorem (Section 9.1.3), requires immediate agreement on operation sequences across Σ. For an integration operation $\phi : D \to D'$, updating d_i, linearizability ensures:

$$\forall q : D \to \{0, 1\}, q(d_i) \text{ reflects } \phi(d_i) \text{ instantly},$$

preserving schema alignment (Section 8.1). However, synchronization delays scale as $O(|N|)$, impacting real-time processing (Section 8.4).

To quantify these trade-offs, we adopt the CAL theorem from Lee et al. [?Lee2023], which relates consistency (C), availability (A), and latency (L) in distributed systems using max-plus algebra, where addition is the maximum operation and multiplication is standard addition. Formally, the CAL theorem states:

$$C + A \leq L,$$

where C measures the time to achieve agreement on dataset states $\text{state}_n(d_i)$, A measures the response time for queries $q(d_i)$, and L encompasses communication and computation latencies across Σ. For linearizable consistency, $C = O(|N|)$, reflecting synchronization delays across $|N|$ nodes, while strong availability requires $A \approx 0$, minimizing response times. In the hypergraph $G = (V, E)$, latency L is influenced by traversal complexity

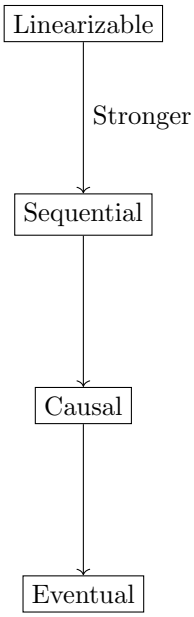

Hierarchy of consistency models [?Jepsen].

FIGURE 10. Relationships between consistency models, from strongest (linearizable) to weakest (eventual).

$O(|E| + |V| \log |V|)$ for navigation queries (Section 3.2). By optimizing L, such as through sparse incidence matrices I_T, I_H (Section 5.2), the data fabric balances C and A, ensuring efficient operations like data integration. In the MTC embedding (Section 5.3), consistency is modeled as morphism composition invariance, with the braiding action c_{X_i,X_j} (Section 5.4) ensuring permutation-invariant updates, mitigating conflicts in distributed environments.

Quantum group actions, such as those of $U_q(\mathfrak{sl}_2)$, could model non-local dependencies in consistency protocols, with their coproduct structure enabling distributed updates that respect hypergraph connectivity, potentially informing novel consensus algorithms as discussed in Section 12.

Eventual consistency permits temporary discrepancies, with replicas of d_i converging over time:

$$\lim_{t\to\infty} \text{state}_n(d_i, t) = \text{state}_m(d_i, t),$$

aligning with scalability goals (Section 8.2). The hypergraph G facilitates eventual consistency by encoding dependencies via hyperedges, enabling navigation to verify convergence. Metadata descriptors $m_j = (d_i, \alpha_j, \tau_j) \in M$ track transformation histories τ_j, ensuring semantic consistency during integration.

9.1.2. *Availability.* Availability guarantees that the data fabric responds to user requests, essential for metadata-driven navigation (Section 3.2) and real-time analytics (Section 8.4). Formally, a system is:

- *Weakly available* if it responds eventually under normal conditions:
$$\forall q : D \to \{0, 1\}, \exists t, q(d_i, t) \text{ returns a result.}$$
- *Strongly available* if it responds during failures or partitions (Section 9.1.3):
$$\forall q, \exists n \in N, q(d_i) \text{ succeeds despite } |N_{\text{failed}}| > 0.$$

The CAL theorem quantifies availability through response time A, where strong availability implies $A \approx 0$, achievable by leveraging redundant paths in G:

$$|\text{Paths}(v_i, v_j)| > 1, \quad v_i, v_j \in V,$$

computed via incidence matrices I_T, I_H in $O(|E|)$ (Section 5.2). For example, a navigation query $q(d_i)$ succeeds if alternative paths exist, with complexity $O(|E| + |V| \log |V|)$. Governance policies P (Section 2.5) enforce

access control without compromising availability, using distributed protocols with complexity $O(|P| \cdot \log |N|)$ (Section 8.3), optimized by minimizing A through edge-based processing. In $\mathcal{DF}$, availability corresponds to the existence of morphisms for query resolution, supported by natural transformations ensuring consistent routing across distributed representations (Section 4.4).

9.1.3. *Partition Tolerance.* Partition tolerance enables the data fabric to function when Σ is partitioned into disconnected components, isolating subsets of nodes N. Formally, Σ is partition-tolerant if:

$$\forall P_1, P_2 \subseteq N, P_1 \cup P_2 = N, P_1 \cap P_2 = \emptyset, \exists D_{P_1}, D_{P_2} \text{ s.t. } \text{ops}(D_{P_1}), \text{ops}(D_{P_2}) \text{ succeed},$$

where ops are operations like queries or updates. The hypergraph G supports partition tolerance by identifying alternative paths, with redundancy:

$$\text{rank}(I_T + I_H) \geq |V|,$$

ensuring connectivity (Section 5.2). The CAL theorem informs partition tolerance by quantifying latency L during partitions, where operations on D_{P_1} and D_{P_2} succeed if:

$$L \geq \max(C_{P_1}, A_{P_1}) + \max(C_{P_2}, A_{P_2}),$$

reflecting independent processing within partitions. Policies P enforce compliance during partitions, restricting sensitive data access (Section 8.3), with complexity $O(|P| \cdot \log |N|)$. Partitioning $D = \bigcup_{n \in N} D_n$ minimizes dependencies, aligning with MTC tensor product decompositions (Section 5.3), where tensor products $X_i \otimes X_j$ model independent data assets.

The tensor product decompositions in the MTC, driven by quantum group fusion rules, could model non-local partition dependencies, enabling quantum-inspired routing strategies that enhance fault tolerance across disconnected components, as proposed for future exploration in Section 12.

Theorem 32. *The CAP theorem asserts that a distributed system cannot simultaneously guarantee linearizable consistency, strong availability, and partition tolerance; at most two properties can be satisfied.*

Proof. Assume a system guarantees all three properties. Consider a partition splitting N into N_1, N_2, with $d_i \in D$ replicated on nodes $n_1 \in N_1$, $n_2 \in N_2$. An update $u(d_i)$ on n_1 must be reflected instantly (linearizable consistency, $C = 0$) and accessible (strong availability, $A = 0$). Partition tolerance requires n_2 to respond, but without communication, n_2 cannot reflect $u(d_i)$, violating consistency, or must reject the request, violating availability. The CAL theorem quantifies this, as $C + A \leq L$, and $L = \infty$ during partitions implies a contradiction if $C = A = 0$. Thus, at most two properties hold, as formalized in [?GilbertLynch2002]. □

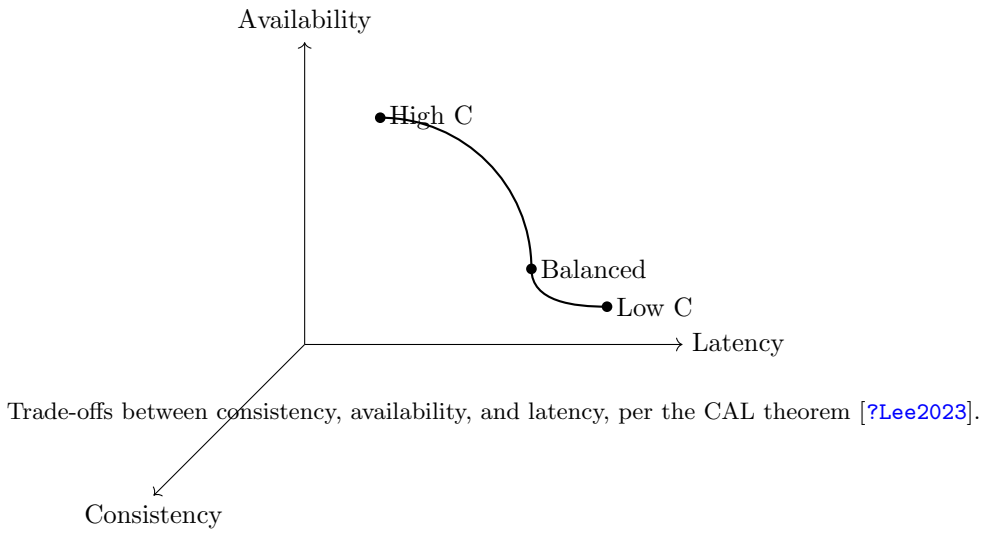

Trade-offs between consistency, availability, and latency, per the CAL theorem [?Lee2023].

FIGURE 11. CAL theorem trade-offs for the data fabric.

The CAP theorem, augmented by the CAL theorem, shapes operations:

Data Integration: Linearizable consistency ($C = O(|N|)$) ensures precise schema alignment for $\phi : D \to D'$, but increases latency L, impacting real-time processing (Section 8.4).
Scalability: Partition tolerance supports distributed analytics $a(D) = \bigoplus_{n \in N} a(D_n)$, with eventual consistency reducing C, minimizing L (Section 8.2).
Real-Time Processing: Strong availability ($A \approx 0$) prioritizes rapid query responses, critical for latency bounds δ, balanced by optimizing L (Section 8.4).

Latency-consistency trade-offs, analyzed in [?Abadi2010, ?Lee2023], influence navigation efficiency via G.

9.1.4. *Completeness.* Completeness ensures that D encompasses all datasets required to satisfy a query $q : D \to \{0, 1\}$:

$$\exists d_i \in D, q(d_i) = 1.$$

Metadata $m_j = (d_i, \alpha_j, \tau_j) \in M$ catalogs attributes and transformation histories, enabling navigation (Section 3.2) to verify coverage. The hypergraph G connects datasets to metadata via hyperedges, ensuring:

$$\forall q, \exists v_i \in V, v_{m_j} \in V, e = (\{v_i\}, \{v_{m_j}\}) \in E, q(v_i) = 1.$$

Provenance tracking (Section 3.5) verifies that transformations $t \in T$ preserve completeness:

$$\text{trace}(d_j) = \{t_k \in T \mid t_k \text{ applied to } d_j\},$$

preventing data loss. In dynamic fabrics, completeness is maintained by updating M, with complexity $O(|M| \cdot |T|)$ (Section 2.2). In $\mathcal{DF}$, completeness corresponds to object coverage, with natural transformations ensuring query-relevant morphisms exist (Section 4.4).

9.1.5. *Causality.* Causality enforces a partial order $\prec$ within G, where $d_i \prec d_j$ if d_i influences d_j via a transformation $t \in T$:

$$d_i \prec d_j \iff \exists t \in T, t(d_i) = d_j \text{ or } \exists e = (\{v_i, \dots\}, \{v_j\}) \in E.$$

Queries respect this order:

$$q(d_j) \implies \text{check } \{d_i \mid d_i \prec d_j\}.$$

Provenance tracking reconstructs τ_j, with hyperedges encoding $\prec$, ensuring causal consistency:

$$\text{state}(d_j, t) \text{ reflects } \{\text{state}(d_i, t') \mid d_i \prec d_j, t' \leq t\}.$$

This supports federated learning (Section 3.6), where local models θ_n depend on causally related D_n. The MTC's braiding action ensures permutation-invariant compositions, preserving dependency structures via:

$$f_e \circ c_{X_i, X_j} = f_e,$$

with complexity $O(|E|)$ (Section 5.4).

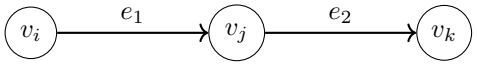

Causal path $v_i \prec v_j \prec v_k$ in G.

FIGURE 12. Causal dependencies in the hypergraph G, with hyperedges e_1, e_2 encoding $\prec$.

Lemma 5. *Causal consistency ensures query results respect the partial order $\prec$, with verification complexity $O(|E|)$.*

Proof. For a query $q(d_j)$, verify $\{d_i \mid d_i \prec d_j\}$ by traversing hyperedges $e \in E$ where $v_j \in H_e$. Each vertex v_j has $|\text{In}(v_j)| \leq O(\log |V|)$ incoming hyperedges (Section 5.2), and traversing all relevant $e \in E$ takes $O(|E|)$. The MTC's braiding ensures invariance, preserving the order's semantics. □

9.1.6. *Fault Tolerance.* Fault tolerance extends partition tolerance to handle node failures in N, ensuring operational continuity. Consensus protocols like Paxos or Raft [?Kleppmann2015] maintain updates to D, with complexity $O(|N|\log|N|)$, supporting consistency during failures. Fault tolerance enables:

- *Governance*: Policies P reroute access requests $r(d_i)$ to available nodes, with complexity $O(|P|\cdot\log|N|)$ (Section 8.3).
- *Navigation*: G redirects queries via redundant paths, computed in $O(|E|+|V|\log|V|)$ (Section 3.2).
- *Analytics*: Federated learning aggregates surviving θ_n, with complexity $O(|\theta_n|\cdot|D_n|)$ (Section 3.6).

The hypergraph's sparse incidence matrices optimize path redundancy:

$$\operatorname{rank}(I_T I_H^T) \geq |V| - |N_{\text{failed}}|,$$

though consensus introduces latency, conflicting with real-time constraints (Section 8.4). Metadata M tracks node status, informing rerouting in $O(|M|)$. The MTC's S-matrix quantifies connectivity, suggesting spectral methods for fault-tolerant routing (Section 5.3).

For more details, see [?Abadi2010, ?Abadi2012, ?Brewer2012, ?GilbertLynch2002, ?GilbertLynch2012, ?Kleppmann2015, ?Viotti2016, ?Lee2023].

10. Practical Implementation: Applying the Data Fabric Framework to a Multi-Component Architecture

The data fabric framework, defined as a tuple $\mathcal{F} = (D, M, G, T, P, A)$ over a distributed system $\Sigma = (N, C)$ (Section 2), provides a robust mathematical structure for managing heterogeneous data ecosystems. Grounded in the hypergraph $G = (V, E)$ (Section 5.2) and unified through the categorical lens of $\mathcal{DF}$ (Section 4.2), the framework supports operations like data integration, metadata-driven navigation, and federated learning (sections 3.1, 3.2 and 3.6). The modular tensor category (MTC) embedding (Section 5.3), enriched by quantum group representations (Section 6) and string theory's topological analogies (Section 7), models relational dynamics with braiding and knot invariants. Consistency, completeness, and causality (Section 9) ensure operational coherence. This section applies the framework to a practical architecture comprising row- and column-oriented databases, real-time analytics, search indices, changelogs, a data warehouse, a view/controller, and transformation pipelines. We formalize component integration within $\mathcal{F}$, derive vector representations using quantum group modules and D-brane analogies, and optimize hypergraph operations with braided structures, addressing scalability and leveraging strategies from Section 8. Visualizations in figs. 13 and 14 enhance the exposition.

10.1. **Architecture Components and Mapping to the Data Fabric.** The architecture comprises components mapped to elements of $\mathcal{F}$ and Σ, integrating algebraic insights from quantum group representations (Section 6) and topological perspectives from string theory (Section 7). These mappings align with the hypergraph G, categorical morphisms in $\mathcal{DF}$, and distributed system dynamics (Section 2.7).

(1) *Row-Oriented Database*: Stores records as tuples $(pk, a_1, a_2, \dots)$, mapping to data assets $D = \{d_i(t)\}_{i,t}$ with schemas $S_i \subseteq \mathcal{A}$ (Section 2.1). Each dataset $d_i(t) : T \to \Omega_i$, with

$$\Omega_i \subseteq \mathbb{R}^k \times \mathcal{C},$$

is a D-brane in data space, with vector representations as $U_q(\mathfrak{sl}_2)$-modules (Section 6). Hosted on nodes $n \in N$, it supports integration queries via intertwiners in $\mathcal{DF}$.

(2) *Column-Oriented Database*: Manages time-series as $(pk : \text{col} : \text{ts}, a_1)$, mapping to D with schemas $S_i = \{pk, \text{col}, \text{ts}, a_1\}$. Temporal attributes $\text{ts} \in \mathbb{R}_{\geq 0}$ define D-brane dynamics, with module structures for temporal queries, hosted on $n \in N$.

(3) *Real-Time Analytics Database*: Computes aggregations over time spans (t_a, t_b) using a Haar basis, mapping to analytical functions $A = \{a_i : D \to \mathbb{R}^k\}$ and metadata M for indexing (sections 2.2 and 2.6). Analytics are modeled as morphisms in $\mathcal{C}$, with braided symmetries ensuring coherence, hosted on specialized nodes in Σ.

(4) *Search Indices*: Forward $(d_i \to \alpha_j)$ and inverted $(\alpha_j \to \{d_i\})$ indices map to metadata

$$M = \{m_j = (d_i, \alpha_j, \tau_j)\},$$

enabling navigation via hyperedges as strings (Section 7). Metadata representations are direct sums of $U_q(\mathfrak{sl}_2)$-modules.

(5) *Changelog*: A sequence of mutations maps to transformation histories

$$\tau_j : D \to \mathcal{H},$$

where $\mathcal{H} = \{(t_k, t_{\text{apply}})\}$, supporting provenance as braided paths (Section 3.5).

(6) *Data Warehouse*: Stores historical records, a subset of D, with metadata M, modeled as static D-branes, hosted on $n \in N$.

(7) *View and Controller*: Manages query routing and authentication, mapping to governance policies $P = \{p_i = (c_i, a_i)\}$ (Section 2.5), ensuring secure execution across Σ.

(8) *Transformation Pipelines*: Apply transformations

$$t_i : \Omega_i \to \Omega_j \in T,$$

recorded in τ_j, as intertwiners or strings connecting D-branes, supporting integration and analytics.

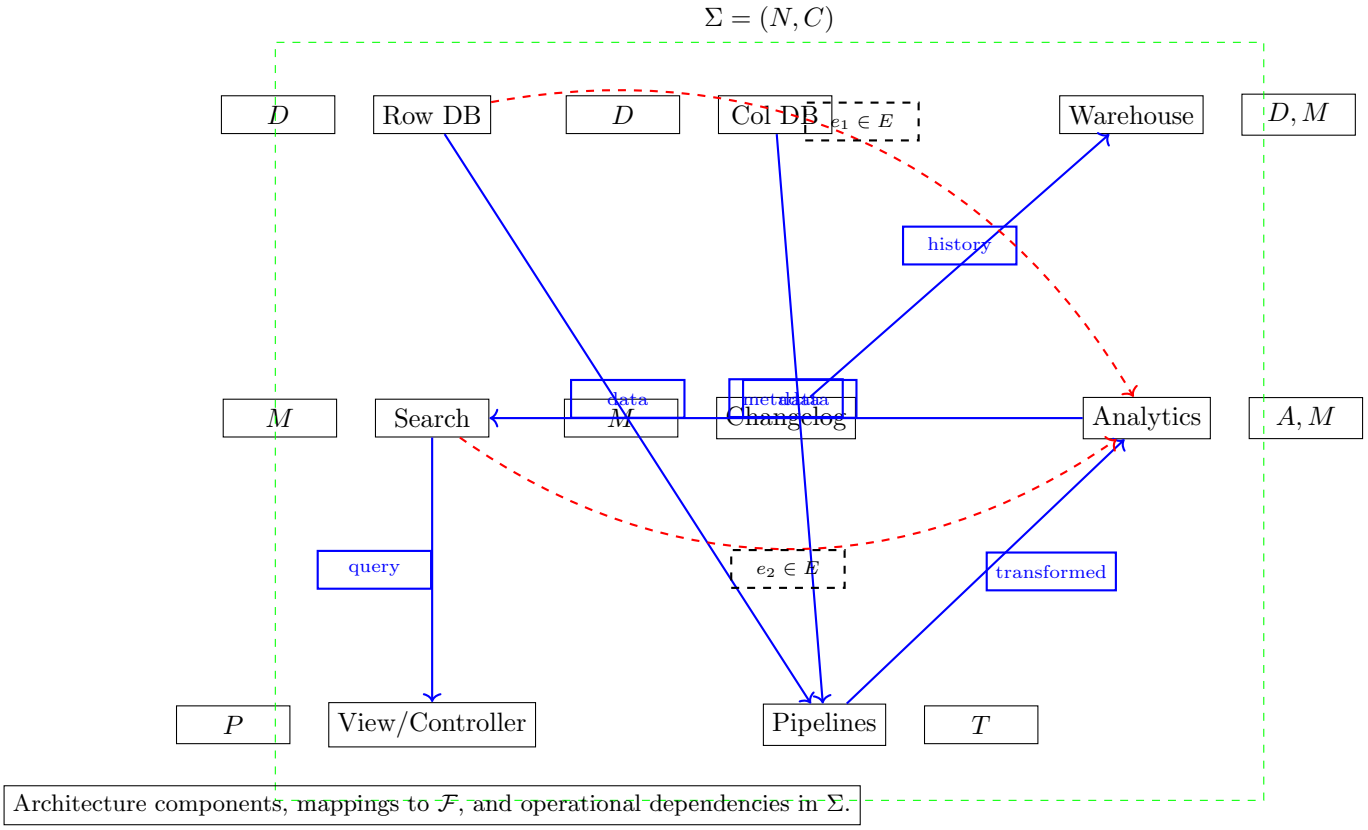

FIGURE 13. Multi-component architecture, with components mapped to data fabric elements D, M, T, P, A, hyperedges $e_1, e_2 \in E$ of G, and hosted in distributed system Σ.

The diagram in fig. 13 illustrates the multi-component architecture of the data fabric framework, which organizes and processes data across a distributed system. The framework is mathematically structured as a tuple $\mathcal{F} = (D, M, G, T, P, A)$, where:

- D: Data assets, such as databases storing raw or processed data.
- M: Metadata, providing information about the data for navigation and tracking.
- G: A hypergraph, modeling complex relationships between components via hyperedges.
- T: Transformations, processes that modify or move data.
- P: Policies, rules governing access and query management.
- A: Analytics, tools for data analysis and insight generation.

The diagram includes eight key components, each mapped to one or more elements of $\mathcal{F}$:

- **Row DB** and **Col DB**: Row-oriented and column-oriented databases, respectively, both corresponding to D, storing raw data.
- **Warehouse**: A data warehouse, mapped to D and M, storing historical data and metadata.
- **Search**: A search index, corresponding to M, which uses metadata to enable fast data retrieval.
- **Changelog**: Tracks changes to data, also mapped to M, and sends historical updates to the Warehouse.
- **Analytics**: A real-time analytics database, mapped to A and M, processing data and generating metadata.
- **View/Controller**: Manages user queries and access, corresponding to P, ensuring secure and policy-compliant operations.
- **Pipelines**: Handles data transformations, mapped to T, converting raw data into formats suitable for analysis.

Data Flows (Solid Arrows): These arrows represent the movement of data or information between components:

- "Data" flows from Row DB and Col DB to Pipelines, where it is processed.
- "Transformed data" is sent from Pipelines to Analytics for real-time analysis.
- "Metadata" generated by Analytics is passed to Search for indexing.
- "Queries" from Search are routed through View/Controller for user access.
- "History" from Changelog is stored in the Warehouse for long-term record-keeping.

Hyperedges (Dashed Arrows): These represent complex relationships in the hypergraph G, connecting multiple components:

- e_1: Links Row DB to Analytics, indicating that analytics operations directly utilize row-oriented data.
- e_2: Links Search to Analytics, showing that metadata from Search supports analytics processes.

The entire architecture is hosted within a distributed system $\Sigma = (N, C)$, where N represents the set of computing nodes (e.g., servers) and C the communication links between them. This distributed setup ensures the system can scale and remain fault-tolerant, with components spread across multiple machines. This diagram encapsulates the data fabric's ability to integrate, transform, and analyze data while maintaining governance and scalability, all within a mathematically rigorous framework.

These components integrate into $\mathcal{F}$, with D as D-branes, M as module sums, T as strings or intertwiners, P enforcing access, A as braided morphisms, and G as a braided worldsheet. The distributed system Σ hosts components across nodes N, with links C enabling data exchange, ensuring consistency and availability (sections 9.1.1 and 9.1.2).

10.2. **Vector Representations and Dimensionality.** Data assets and metadata are represented as vectors in finite-dimensional spaces (Section 5.1), enhanced by quantum group modules (Section 6) and D-brane coordinates (Section 7). For a dataset $d_i(t) \in D$, with schema S_i comprising numerical attributes $\mathbf{x}_{\text{num}} \in \mathbb{R}^k$, categorical attributes $\{c_{j_1}, \ldots, c_{j_l}\}$ embedded via $\phi : \mathcal{C} \to \mathbb{R}^d$, and temporal attributes $\text{ts} \in \mathbb{R}$, the vector is:

$$\mathbf{v}_i(t) = (\mathbf{x}_{\text{num}}, \phi(c_{j_1}), \ldots, \phi(c_{j_l}), \text{ts}) \in \mathbb{R}^{k+ld+1}.$$

This defines a $U_q(\mathfrak{sl}_2)$-module $V_i \cong \mathbb{C}^{k+ld+1}$, with $\rho_i : U_q(\mathfrak{sl}_2) \to \text{End}(V_i)$ acting via generators E, F, K. Metadata $m_j = (d_i, \alpha_j, \tau_j) \in M$ has:

$$\mathbf{v}_{m_j} = (\phi(\alpha_j), \mathbf{v}_{\tau_j}) \in \mathbb{R}^{q+s},$$

forming a module $V_{m_j} \cong \mathbb{C}^{q+s}$. As D-branes, $\mathbf{v}_i(t)$ and $\mathbf{v}_{m_j}$ specify positions in data space, with schemas as boundary conditions.

Assuming $k = 2$, $l = 2$, $d = 2$, $q = 2$, $s = 2$, and one temporal attribute:

$$\dim = 2 + (2 \cdot 2) + 1 + 2 + 2 = 11,$$

ranging from 6 to 15. In G, vertices use $\mathbf{v}_i(t) \in \mathbb{R}^{11}$, with incidence matrices $I_T, I_H \in \{0,1\}^{|V|\times|E|}$ encoding string-like hyperedges. Cosine similarity:

$$\cos(\mathbf{v}_i, \mathbf{v}_j) = \frac{\mathbf{v}_i \cdot \mathbf{v}_j}{\|\mathbf{v}_i\|_2 \|\mathbf{v}_j\|_2},$$

computed in $O(11)$, is enhanced by quantum algorithms on V_i, V_j, leveraging braiding c_{X_i,X_j} for symmetry-invariant clustering (sections 6 and 7).

Example 10. *For a sales dataset $d_1(t) \in D$ (schema $S_1 = \{price, quantity\}$), $\mathbf{v}_1(t) \in \mathbb{R}^2$ forms a module $V_1 \cong \mathbb{C}^2$ (spin-1/2 representation) and a D-brane D_1. A transformation to inventory $d_2(t)$ is an intertwiner $t_1 : V_1 \to V_2$ and a string from D_1 to D_2, with braiding ensuring order-invariant similarity searches.*

10.3. **Hypergraph Construction and Role in Operations.** The hypergraph $G = (V, E)$ connects D and M, with vertices $V = D \cup M$ as D-branes and hyperedges $E \subseteq \mathcal{P}(V)$ as strings. Hyperedges are formed based on:

- *Integration*: Transformations $t_i : \{d_{i_1}, \dots, d_{i_n}\} \to d_j \in T$, as intertwiners $t_i : \otimes V_{i_k} \to V_j$, induce $e = (\{v_{i_1}, \dots, v_{i_n}, v_{m_k}\}, \{v_j\})$, with $m_k \in M$ recording t_i.
- *Navigation*: Shared attributes $\alpha_k \subseteq \mathcal{A}$ induce $e = (\{v_i, v_j\}, \{v_{m_k}\})$, with paths as braided worldsheets (Section 7).
- *Provenance*: Sequences induce $e = (\{v_{i_1}, \dots, v_{i_n}, v_{m_j}\}, \{v_j\})$, tracing lineage as braided paths.

Incidence matrices I_T, I_H ensure sparsity ($|E| = O(|V| \log |V|)$). Navigation queries traverse paths $(e_1, e_2, \dots)$ using Dijkstra's algorithm:

$$\text{time} = O(|E| + |V| \log |V|),$$

with braiding c_{X_i, X_j} ensuring permutation invariance. The braid group B_n representation $\pi(\sigma_i) = c_{X_i, X_{i+1}}$ models path crossings, detecting anomalies via knot invariants (Section 7).

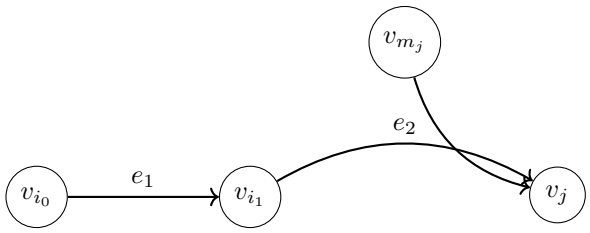

Hyperedge path e_1, e_2 as a braided worldsheet, tracing v_j to v_{i_0}.

FIGURE 14. Hypergraph G connectivity, with paths as strings for provenance tracking from dataset v_j to sources v_{i_0}, v_{i_1}.

Example 11. *A provenance query traces a forecast $d_j(t)$ to sales $d_{i_0}(t)$ and inventory $d_{i_1}(t)$ via e_1, e_2. The path forms a braid in B_3, with $\sigma_1 \mapsto c_{X_{i_0}, X_{i_1}}$. A non-trivial Jones polynomial flags a cycle, guiding pipeline optimization.*

10.4. **Operations in the Architecture.** The architecture supports operations, formalized with quantum group and string theory insights:

(1) *Data Integration*: Transformations $t_i \in T$, as intertwiners $t_i : \otimes V_{i_k} \to V_j$, align schemas, encoded as strings from D-branes D_{i_k} to D_j. Braiding ensures order invariance, addressing heterogeneity (Section 8.1).
(2) *Metadata-Driven Navigation*: Queries traverse G as braided worldsheets, using B_n representations, with complexity $O(|E| + |V| \log |V|)$ (Section 3.2).
(3) *Provenance Tracking*: Transformation histories $\tau_j(d_j)$ are reconstructed via hyperedges, with knot invariants detecting cycles in $O(|E| \cdot n \cdot 2^n)$ (sections 3.5 and 7).

Example 12. *Integrating sales and inventory datasets uses an intertwiner $t_1 : V_1 \otimes V_2 \to V_3$, aligning D-branes D_1, D_2 to D_3. Braiding c_{X_1, X_2} ensures robust schema matching, with a Jones polynomial check for pipeline cycles.*

10.5. **Scalability and Performance Considerations.** The architecture leverages quantum and string-theoretic insights for scalability:

- *Partitioning*: Datasets are partitioned across N, using spectral clustering on the Laplacian $L = I_T I_T^T - I_H I_H^T$ or S-matrix, enhanced by $U_q(\mathfrak{sl}_2)$ fusion rules (Section 6), and geometric alignment of D-branes (Section 7), with complexity $O(|V| \log |V|)$.
- *Parallel Processing*: Local computations on $n \in N$ reduce to $O(|D_n|)$, with braided paths parallelizing federated learning (Section 3.6).

- *Efficient Traversal*: Sparse G ensures navigation scales as $O(|E| + |V| \log |V|)$, with braid-based routing enhancing fault tolerance (Section 9.1.3).

Lemma 6. *Hypergraph traversal for query resolution, modeled as braided worldsheets, has complexity* $O(|E| + |V| \log |V|)$*, preserved under sparse partitioning.*

Proof. For a query q, traverse paths in G using a hypergraph-adapted Dijkstra's algorithm, with edges as strings. With $|E| = O(|V| \log |V|)$, edge traversal is $O(|E|)$, and priority queue updates are $O(|V| \log |V|)$. Braiding c_{X_i,X_j} ensures permutation invariance, and partitioning maintains sparsity ($|E_n| = O(|V_n| \log |V_n|)$), yielding $O(|E| + |V| \log |V|)$ (sections 7 and 8.2). □

Quantum-inspired partitioning, using the S-matrix and fusion rules, and geometric D-brane alignment optimize load balancing, as proposed in Section 12.

This section applies the data fabric framework $\mathcal{F}$ to a multi-component architecture, integrating quantum group representations and string theory's topological insights. Components map to D-branes and modules, vectors leverage braided modules, and operations use strings and braids for coherence and anomaly detection. The architecture ensures scalability, addressing challenges from Section 8 and maintaining consistency, completeness, and causality (Section 9), bridging theory and practice for advanced data ecosystems.

11. A Physics Model: A 4D Spacetime Manifold for Data Fabrics

To provide a rigorous foundation for our data fabric framework, we introduce a physics-inspired model based on a 4D spacetime manifold $\mathcal{M}$. This model captures the spatial and temporal dynamics of the distributed system $\Sigma = \langle N, C \rangle$, addressing key challenges such as causality, consistency, and scalability. By representing nodes N, datasets D, and transformations T geometrically, the manifold offers a unified framework to optimize operations like data integration (Section 3) and real-time processing (Section 8). We define $\mathcal{M}$ as a Riemannian manifold, study its embedding into Euclidean space, and connect it to the hypergraph G and categorical structure $\mathcal{DF}$.

11.1. Defining the 4D Spacetime Manifold $\mathcal{M}$.

Definition. 33. *A* data fabric manifold *is a connected, smooth 4-dimensional Riemannian manifold* $(\mathcal{M}, g)$*, where* g *is a smooth, positive-definite metric tensor of type* $(0, 2)$*. We assume*

$$\mathcal{M} \cong \mathbb{R}^3 \times \mathbb{R}, \quad \text{with local coordinates } (x^1, x^2, x^3, t),$$

and metric

$$g = g_{ij}(x, t)\, dx^i dx^j + g_{00}(x, t)\, dt^2,$$

where $i, j = 1, 2, 3$*.*

Remark 1. *The spatial coordinates* x^1, x^2, x^3 *represent logical or physical locations of nodes* $n \in N$ *(e.g., data centers), while* t *encodes the temporal evolution of datasets* $d_i(t) \in D$*. The metric* g *quantifies system properties such as network latency or computational load, enabling optimization of data fabric operations.*

The manifold $\mathcal{M}$ integrates the data fabric tuple $\mathcal{F} = \langle D, M, G, T, P, A \rangle$ by mapping its components to geometric entities. Datasets $d_i(t) \in D$ are points $p \in \mathcal{M}$, nodes $n \in N$ correspond to spatial coordinates (x^1, x^2, x^3), and communication links $(n_i, n_j) \in C$ are modeled as curves with lengths determined by g. The hypergraph $G = \langle V, E \rangle$ is embedded such that vertices $V = D \cup M$ are points, and hyperedges $e \in E$ are causal paths reflecting multi-way relationships (Section 5). The metric g is constructed to reflect Σ's dynamics: spatial components $g_{ij}(x, t)$ are derived from the adjacency matrix A_Σ, where $g_{ij} \propto w(n_i, n_j)$ (latency or bandwidth, Section **??**), and the temporal component $g_{00}(x, t) \propto \text{load}(n) = |D_n| + \sum_{a_i \in A_n} \text{cost}(a_i)$ captures processing delays. This formulation grounds $\mathcal{M}$ in the data fabric's operational context, facilitating analysis of consistency (Section 9) and scalability (Section 8).

11.2. Embedding $\mathcal{M}$ into Euclidean Space.

Theorem 34 (Nash Embedding Theorem)**.** *Let* $(\mathcal{M}, g)$ *be a smooth, compact Riemannian 4-manifold. Then there exists an isometric embedding*

$$\varphi : \mathcal{M} \hookrightarrow \mathbb{R}^d, \quad \text{for some } d \geq 14,$$

such that $\varphi^* g_{Eucl} = g$*, where* g_{Eucl} *is the Euclidean metric on* $\mathbb{R}^d$*.*

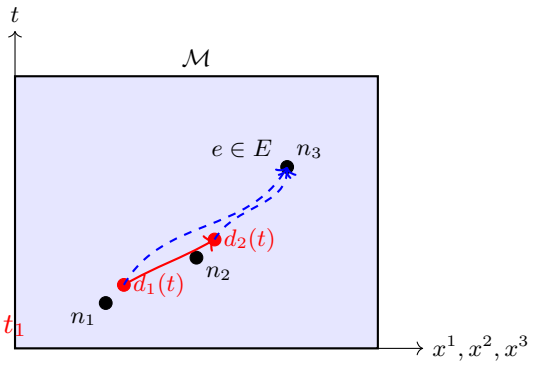

FIGURE 15. Mapping of data fabric components to the 4D manifold $\mathcal{M}$, with nodes $n_i \in N$, datasets $d_i(t) \in D$, transformations $t_1 \in T$, and hyperedges $e \in E$.

Proof. By Nash's isometric embedding theorem [?Nash1956], any smooth n-dimensional Riemannian manifold $(\mathcal{M}, g)$ admits a C^1-isometric embedding into $\mathbb{R}^d$ with $d \geq n(3n+11)/2$. For $n = 4$, compute:

$$d \geq \frac{4 \cdot (3 \cdot 4 + 11)}{2} = \frac{4 \cdot 23}{2} = 46.$$

However, for compact 4-manifolds, refinements by Gromov [?Gromov1986] reduce the dimension. Consider the metric g as a symmetric positive-definite tensor. The embedding $\varphi : \mathcal{M} \to \mathbb{R}^d$ must satisfy:

$$g_{\mu\nu} = \sum_{a=1}^{d} \frac{\partial \varphi^a}{\partial x^\mu} \frac{\partial \varphi^a}{\partial x^\nu},$$

where φ^a are the coordinate functions in $\mathbb{R}^d$, and $g_{\mu\nu}$ are the components of g. This forms a system of $n(n+1)/2 = 4 \cdot 5/2 = 10$ partial differential equations (PDEs) for the d-components of φ. For $d \geq n(n+1)/2 + 2n = 10 + 8 = 18$, the system is overdetermined, allowing a solution via iterative perturbation methods [?Nash1956]. Further optimizations for 4-manifolds, leveraging compactness, reduce $d \geq 14$ for C^1-embeddings [?Gromov1986]. The embedding preserves g, ensuring $\varphi^* g_{\text{Eucl}} = g$. □

The embedding $\varphi : \mathcal{M} \hookrightarrow \mathbb{R}^{14}$ enables efficient computations by representing the manifold's geometry in Euclidean space. In the context of the data fabric, datasets $d_i(t) \in D$ are modeled as D-branes in $\mathcal{M}$, with schemas S_i as boundary conditions, and transformations $t_i \in T$ or hyperedges $e \in E$ as open strings connecting them (Section 7). The manifold $\mathcal{M}$ acts as a worldsheet-like space where strings propagate, with the metric g quantifying interaction costs (e.g., latency $w(n_i, n_j)$ or computational load $\text{load}(n)$). The embedding maps D-branes and strings to $\mathbb{R}^{14}$, allowing Euclidean algorithms (e.g., vector distance calculations in $O(14)$) to optimize operations like data integration (Section 3) or anomaly detection via knot invariants (Section 7).

This string theory perspective reimagines the data fabric as a physical system. Datasets, as D-branes, are positioned at points $p_i = (x_i^1, x_i^2, x_i^3, t) \in \mathcal{M}$, with coordinates reflecting their hosting node $n_i \in N$ and timestamp. Transformations $t_i : \Omega_i \to \Omega_j$ are strings stretching between D-branes, with the energy functional

$$E(\gamma) = \int_0^1 g(\dot{\gamma}, \dot{\gamma})\, ds$$

(see Section 11.3) measuring their computational cost. Hyperedges, such as $e = (\{d_1, m_1\}, \{d_2\})$, form braided configurations, enabling topological analysis (e.g., Jones polynomial) to detect cycles or anomalies in data pipelines (Section 7). The embedding into $\mathbb{R}^{14}$ maps these structures to a higher-dimensional space, where string interactions are computed efficiently, supporting scalability (Section 8) and causal consistency (Section 9).

Remark 2. *The string theory analogy connects to the modular tensor category (MTC) framework (Section 5), where braiding actions c_{X_i,X_j} model string crossings. Future work could explore closed strings for global analytics $a_i \in A$ or quantum group actions (Section ??) to quantify non-local dependencies, enhancing fault tolerance (Section 9).*

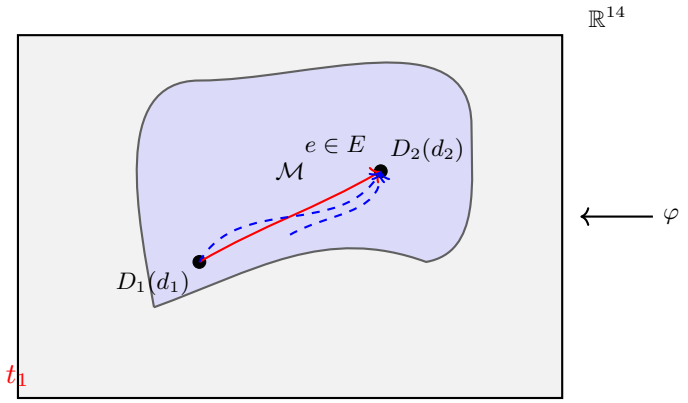

FIGURE 16. Isometric embedding of the 4D manifold $\mathcal{M}$ into $\mathbb{R}^{14}$. Datasets $d_1, d_2 \in D$ are D-branes D_1, D_2, with schemas as boundary conditions. Transformations $t_1 \in T$ are open strings, and hyperedges $e \in E$ are braided strings, forming a worldsheet-like structure in $\mathcal{M}$. The embedding φ preserves the metric g, enabling efficient computations of string interactions for data fabric operations.

11.3. **Geometric Representation of Data.** We model system elements as geometric entities:

- **Datasets:** Points $p \in \mathcal{M}$, whose coordinates (x^1, x^2, x^3, t) reflect the hosting node $n \in N$ and timestamp of $d_i(t) \in D$.
- **Transformations:** Curves $\gamma : [0,1] \to \mathcal{M}$ representing data workflows, e.g., $t_i \in T$ mapping $d_i(t)$ to $d_j(t)$.
- **Causal Relations:** A partial order $p \prec q$ iff there exists a causal path from p to q, encoding dependencies in G.

Causal paths in $\mathcal{M}$ model transformations T and provenance tracking (Section 3). A sequence $t_1, t_2 \in T$, e.g.,

$$d_1 \xrightarrow{t_1} d_2 \xrightarrow{t_2} d_3,$$

is a path γ connecting points $p_1, p_2, p_3 \in \mathcal{M}$, with $\frac{d\gamma^0}{ds} > 0$ ensuring temporal order (Section 9). This enforces causality ($d_i \prec d_j$) and aligns with hyperedges $e = (\{d_1, m_1\}, \{d_2\}) \in E$, where metadata $m_1 \in M$ records t_1. The energy functional $E(\gamma)$ quantifies computational or latency costs, supporting optimization of integration (Section 3).

Definition. 35. *Let $\gamma : [0,1] \to \mathcal{M}$ be a smooth path. Define the* operational cost *as the energy functional*

$$E(\gamma) = \int_0^1 g\left(\dot\gamma(s), \dot\gamma(s)\right)\, ds.$$

The associated length functional is

$$L(\gamma) = \int_0^1 \sqrt{g\left(\dot\gamma(s), \dot\gamma(s)\right)}\, ds.$$

Proposition 3. *If γ is a geodesic with respect to the Levi-Civita connection of g, then γ locally minimizes $L(\gamma)$.*

Proof. Consider the length functional $L(\gamma) = \int_0^1 \sqrt{g(\dot\gamma(s), \dot\gamma(s))}\, ds$. A path γ is a geodesic if it is a critical point of the energy functional $E(\gamma) = \int_0^1 g(\dot\gamma(s), \dot\gamma(s))\, ds$, as $E(\gamma) = L(\gamma)^2/2$ for unit-speed curves. The Euler-Lagrange equations for $E(\gamma)$, derived via variational calculus, yield the geodesic equation:

$$\frac{d^2\gamma^\mu}{ds^2} + \Gamma^\mu_{\nu\lambda} \frac{d\gamma^\nu}{ds} \frac{d\gamma^\lambda}{ds} = 0,$$

where $\Gamma^\mu_{\nu\lambda}$ are the Christoffel symbols of the Levi-Civita connection. For a geodesic γ, the second variation of $L(\gamma)$ is positive under small perturbations with fixed endpoints, ensuring γ locally minimizes $L(\gamma)$ [?Lee2018]. □

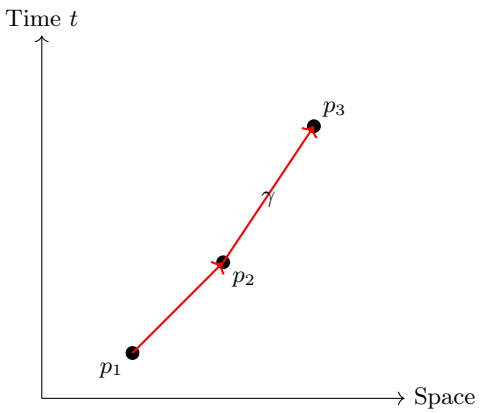

FIGURE 17. Causal path γ connecting events $p_1 \prec p_2 \prec p_3$ in $\mathcal{M}$, representing a transformation sequence.

11.4. **Practical Example.** Consider a data fabric managing IoT sensor data across three nodes $n_1, n_2, n_3 \in N$, located in distinct data centers. Each node logs timestamped events, e.g., temperature readings $d_i(t) \in D$, as points

$$p_i = (x_i^1, x_i^2, x_i^3, t) \in \mathcal{M},$$

where (x_i^1, x_i^2, x_i^3) are geographic coordinates of n_i, and t is the event timestamp. The metric g sets $g_{ij} \propto w(n_i, n_j)$ (network latency from A_Σ) and $g_{00} \propto |D_{n_i}|$.

Embedding $\mathcal{M}$ into $\mathbb{R}^{14}$ via φ, a query propagation from n_1 to n_3 via n_2, e.g., aggregating $d_1(t)$ and $d_2(t)$ into $d_3(t)$, is a curve γ with $\varphi(\gamma) = \{y_1, y_2, y_3\} \in \mathbb{R}^{14}$. The energy

$$E(\gamma) \approx w(n_1, n_2) + w(n_2, n_3)$$

represents total latency. Checking $\frac{d\gamma^0}{ds} > 0$ in $\mathbb{R}^{14}$ (projecting to the time coordinate) takes $O(14)$; a non-monotonic γ^0 (e.g., $t_2 < t_1$) flags a causality violation, detectable by comparing timestamps. This aligns with provenance tracking (Section 3), as the path γ corresponds to a hyperedge $e = (\{d_1, d_2, m_1\}, \{d_3\})$, with $m_1 \in M$ recording the aggregation.

For example, if $d_1(t_1)$ at n_1 (time $t_1 = 2025{-}05{-}09T10:00$) and $d_2(t_2)$ at n_2 (time $t_2 = 2025{-}05{-}09T10:01$) are transformed into $d_3(t_3)$ at n_3 (time $t_3 = 2025-05-09T10:02$), γ connects

$$p_1 = (x_1, t_1), \quad p_2 = (x_2, t_2), \quad p_3 = (x_3, t_3).$$

If $t_3 < t_2$, the system flags a violation, prompting rerouting via alternative nodes to minimize $E(\gamma)$.

11.5. **Toward Higher-Dimensional Models.** To incorporate features like data modalities or governance levels, we generalize to higher-dimensional manifolds:

Theorem 36. *Let $\mathcal{M}^n$ be a smooth, compact Riemannian n-manifold. Then:*

(1) There exists a topological embedding $\mathcal{M}^n \hookrightarrow \mathbb{R}^{2n}$ (Whitney).
(2) There exists an isometric embedding $\mathcal{M}^n \hookrightarrow \mathbb{R}^d$, where $d \geq n(3n+11)/2$ (Nash).

Proof. For (1), the Whitney embedding theorem [?Whitney1944] states that any smooth n-manifold embeds topologically into $\mathbb{R}^{2n}$. A smooth map $f : \mathcal{M}^n \to \mathbb{R}^{2n}$ is constructed such that f is injective and df has full rank, ensuring an embedding.

For (2), Nash's theorem [?Nash1956] guarantees an isometric embedding into $\mathbb{R}^d$ with $d \geq n(3n+11)/2$. For an n-manifold, the metric g is preserved by a C^1-map $\varphi : \mathcal{M}^n \to \mathbb{R}^d$, satisfying $\varphi^* g_{\text{Eucl}} = g$. The dimension bound arises from solving the system of partial differential equations for φ, ensuring the induced metric matches g. For $n = 5$, $d \geq 5 \cdot (3 \cdot 5 + 11)/2 = 65$, though lower bounds (e.g., $d \geq 25$) are possible with advanced techniques [?Gromov1986]. □

Higher-dimensional manifolds $\mathcal{M}^n$ (e.g., $n = 5, 6$) extend the framework. A fifth dimension could represent data modalities (numerical vs. categorical, Section **??**), with coordinates $x^5 \in \{0, 1\}$. A sixth dimension might

encode governance levels from P, e.g., $x^6 \propto c_i(d_i, u)$ (security clearance, Section **??**). The Whitney embedding into $\mathbb{R}^{2n}$ (e.g., $\mathbb{R}^{10}$ for $n = 5$) or Nash embedding into $\mathbb{R}^{25}$ ensures computability, enabling complex relationship modeling in G. These extensions support topological data analysis (Section 12) for dynamic fabrics.

The 4D spacetime manifold $(\mathcal{M}, g)$ provides a geometric framework for the data fabric $\mathcal{F}$, unifying the spatial distribution of Σ and temporal dynamics of D. By embedding $\mathcal{M}$ into $\mathbb{R}^{14}$, we enable efficient computations for optimizing transformations T and ensuring causality (Section 9). The metric g, derived from A_Σ and node loads, quantifies operational costs, addressing scalability (Section 8). Geodesics and causal paths model data workflows and provenance, enhancing integration and real-time processing (Sections 3, 8). Future work could explore curvature analysis to balance loads across N or harmonic forms for data synchronization, aligning with directions in Section 12 for quantum-inspired and topological advancements.

12. Concluding Remarks

The data fabric framework, formalized as the tuple $\mathcal{F} = (D, M, G, T, P, A)$ over a distributed system $\Sigma = (N, C)$, establishes a transformative mathematical paradigm for managing heterogeneous, distributed data ecosystems. This paper has woven together a rich tapestry of theoretical advancements and practical applications, unifying hypergraph-based connectivity, categorical structures, modular tensor categories (MTCs), quantum group representations, and string theory-inspired topological insights. By synthesizing these perspectives, the framework not only addresses the complexities of modern data management but also charts a bold path for future innovation in data-intensive domains.

At its core, the framework's theoretical contributions are anchored in a rigorous algebraic and topological foundation. The hypergraph $G = (V, E)$, with vertices $V = D \cup M$ representing data assets and metadata, encodes multi-way relationships through sparse incidence matrices, enabling efficient navigation and provenance tracking. The categorical structure $\mathcal{DF}$, modeling datasets as objects and transformations as morphisms, provides a unified language for operations such as data integration, metadata-driven navigation, and federated learning. The MTC embedding, with its braided monoidal structure, captures relational symmetries via the braiding action c_{X_i,X_j}, ensuring permutation-invariant operations. These foundational elements, introduced and developed across the paper, address NP-hard challenges like schema matching and partitioning by leveraging spectral methods and symmetry-based alignments.

The introduction of quantum group representations, particularly through $U_q(\mathfrak{sl}_2)$, marks a significant advancement. By modeling datasets as finite-dimensional modules and transformations as intertwiners, the framework captures non-commutative dependencies inherent in distributed systems. The MTC's fusion rules and S-matrix, derived from quantum group representations, enable spectral optimization, reducing the complexity of partitioning to $O(|V| \log |V|)$ and enhancing schema alignment through algebraic symmetries. These insights, detailed in the representation theory section, provide a powerful tool for modeling dynamic data relationships and optimizing computational tasks.

Complementing this algebraic approach, string theory offers a topological and geometric lens that reimagines data fabric operations. Datasets are modeled as D-branes, with schemas as boundary conditions, and transformations as open strings connecting them. Hypergraph paths form braided worldsheets, with the braid group B_n representation $\pi(\sigma_i) = c_{X_i,X_{i+1}}$ encoding data flow symmetries. Knot invariants, such as the Jones polynomial, detect anomalies like cyclic dependencies, providing a novel mechanism for pipeline optimization. These topological analogies, explored in the string theory section, transform heterogeneity into a geometric alignment problem and scalability into a manifold optimization task, enriching the framework's expressive power.

Practically, the framework is realized in a multi-component architecture integrating row- and column-oriented databases, real-time analytics, search indices, changelogs, a data warehouse, a view/controller, and transformation pipelines. This architecture leverages vector representations in $\mathbb{R}^{11}$ as $U_q(\mathfrak{sl}_2)$-modules and D-branes, with hypergraph traversals modeled as braided worldsheets. Operations like data integration and navigation benefit from intertwiners and braid group symmetries, achieving complexities of $O(|E| + |V| \log |V|)$. Scalability is enhanced through quantum-inspired spectral clustering and geometric D-brane alignment, while knot invariants ensure robust anomaly detection. This practical implementation demonstrates the framework's ability to bridge theoretical rigor with real-world applicability, addressing computational challenges and ensuring consistency, completeness, and causality in distributed environments.

Looking forward, the data fabric framework opens exciting avenues for research and deployment. The integration of dynamic monoidal categories could model temporal governance constraints, enhancing policy enforcement in real-time systems. Topological data analysis (TDA), inspired by string theory's TQFT connections, offers potential for detecting concept drift in streaming data, using persistent homology to track evolving distributions. Quantum-inspired algorithms, leveraging the MTC's S-matrix and fusion rules, could achieve sublinear complexities for partitioning and analytics in quantum computing environments. The braid group's role in modeling data flows suggests scalable anomaly detection frameworks, applicable to complex pipelines in IoT, AI, and cloud-based analytics platforms. These directions, building on the paper's algebraic and topological innovations, position the data fabric as a cornerstone for next-generation data management systems.

In conclusion, this work represents a paradigm shift in distributed data management, harmonizing hypergraph connectivity, categorical unification, quantum group representations, and string-theoretic topologies. By addressing heterogeneity, scalability, and real-time processing through a unified mathematical lens, the framework not only resolves critical computational challenges but also lays a foundation for transformative applications. As data ecosystems grow in complexity, the data fabric stands as a beacon of theoretical depth and practical utility, ready to shape the future of large-scale, data-intensive domains.

References

[1] Saunders Mac Lane, *Categories for the working mathematician*, Graduate Texts in Mathematics, vol. 5, Springer-Verlag, New York, NY, 1971.

[2] Steve Awodey, *Category theory*, 2nd ed., Oxford Logic Guides, vol. 52, Oxford University Press, Oxford, UK, 2010.

[3] David I. Spivak, *Category theory for the sciences*, MIT Press, Cambridge, MA, 2014.

[4] Peter Buneman, David A. Holland, and Ryan Schultz, *Categorical data integration for computational science*, Electronic Notes in Theoretical Computer Science **318** (2016), 49–65. Proceedings of the 7th International Workshop on Data Integration in the Life Sciences (DILS 2016).

[5] Vladimir G. Turaev, *Quantum invariants of knots and 3-manifolds*, De Gruyter, 1994.

[6] S. Bakalova and A. Kirillov Jr, *Modular tensor categories and their applications*, Journal of Pure and Applied Algebra **216** (2012), no. 8-9, 1801–1818.

[7] Edward Witten, *Topological quantum field theory*, Communications in Mathematical Physics **117** (1988), no. 3, 353–386.

[8] Jepsen LLC, *Consistency Models*, 2025. [Online; accessed 23. Apr. 2025].

[9] Edward A. Lee, Ravi Akella, Soroush Bateni, Shaokai Lin, Marten Lohstroh, and Christian Menard, *Consistency vs. availability in distributed real-time systems*, arXiv **2301.08906** (2023), available at 2301.08906.

[10] Seth Gilbert and Nancy A. Lynch, *Brewer's conjecture and the feasibility of consistent, available, partition-tolerant web services*, SIGACT News **33** (2002), no. 2, 51–59.

[11] Daniel Abadi, *Problems with CAP, and Yahoo's little known NoSQL system*, 2010. [Online; accessed 22. Apr. 2025].

[12] Martin Kleppmann, *A critique of the cap theorem*, 2015.

[13] Daniel Abadi, *Consistency Tradeoffs in Modern Distributed Database System Design: CAP is Only Part of the Story*, Computer **45** (January 2012), no. 2, 37–42.

[14] Eric Brewer, *CAP twelve years later: How the "rules" have changed*, Computer **45** (January 2012), no. 2, 23–29.

[15] Seth Gilbert and Nancy A. Lynch, *Perspectives on the CAP theorem*, Computer **45** (2012), no. 2, 30–36.

[16] Pietro Viotti and Marko Vukolić, *Consistency in non-transactional distributed storage systems*, ACM Computing Surveys **49** (2016), no. 1, 19:1–19:34.

[17] John Nash, *The imbedding problem for Riemannian manifolds*, Annals of Mathematics **63** (1956), no. 1, 20–63. This paper presents the Nash embedding theorem, proving that any smooth Riemannian manifold can be isometrically embedded into Euclidean space.

[18] Mikhail Gromov, *Partial differential relations*, Ergebnisse der Mathematik und ihrer Grenzgebiete. 3. Folge / A Series of Modern Surveys in Mathematics, vol. 9, Springer-Verlag, Berlin, Heidelberg, 1986. This book includes refinements to embedding theorems, reducing the dimension required for isometric embeddings of compact manifolds.

[19] John M. Lee, *Introduction to Riemannian manifolds*, 2nd ed., Graduate Texts in Mathematics, vol. 176, Springer International Publishing, Cham, Switzerland, 2018. This text provides a comprehensive treatment of Riemannian geometry, including the variational characterization of geodesics.

[20] Hassler Whitney, *The self-intersections of a smooth n-manifold in 2n-space*, Annals of Mathematics **45** (1944), no. 2, 220–246. This paper establishes the Whitney embedding theorem, showing that any smooth n-manifold can be embedded into $\mathbb{R}^{2n}$.